

ECT* workshop - "New perspectives in the charge radii determination for light nuclei"



TPE corrections to muonic atoms from lattice QCD

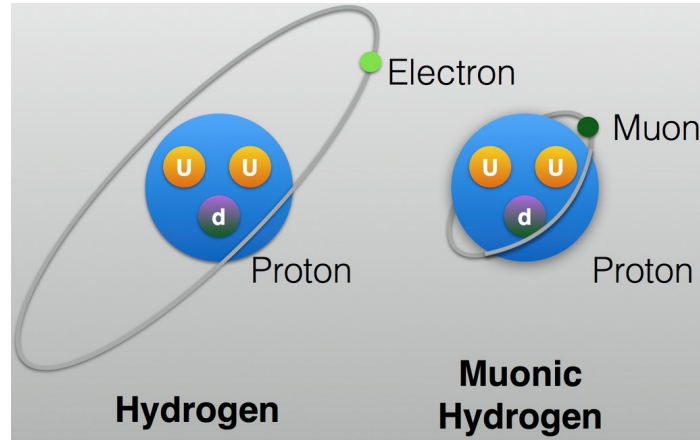
Xu Feng (Peking University)

2025.08.01

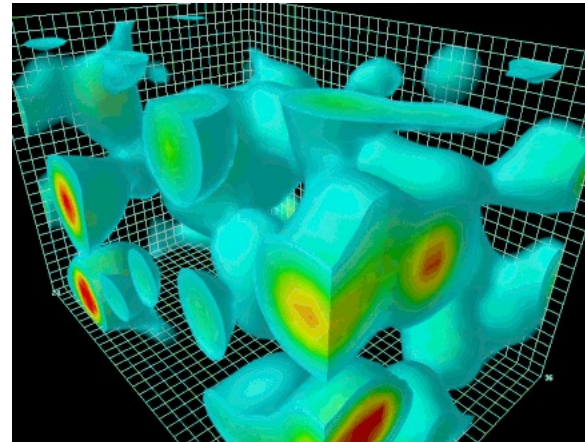
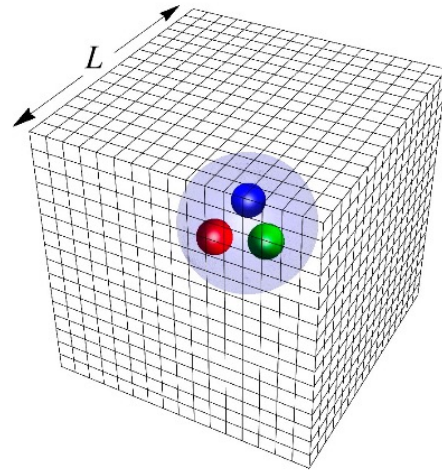


Why muonic atom

- Muonic atoms are exotic atoms

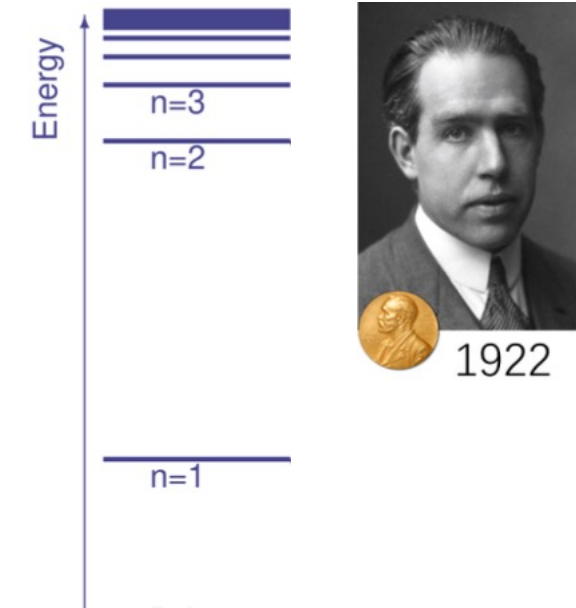


- We are using lattice QCD to study the strong interaction in the non-perturbative regime. Why muonic atoms?



- Let us start with the simplest atom system – the hydrogen

Hydrogen Spectroscopy

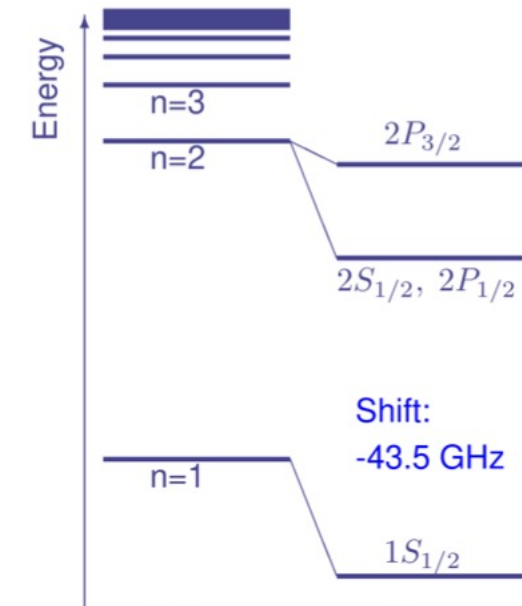


- Bohr model predicts the hydrogen spectroscopy

$$E = -\frac{R_{\infty}}{n^2}$$

- Assume:
 - ① proton mass infinitely large
 - ② only Coulomb interaction
 - ③ no QED or QCD corrections

Rydberg constant is given by $R_{\infty} \approx \frac{\alpha^2 m_e}{4\pi}$



- Dirac theory predicts the fine structure splitting

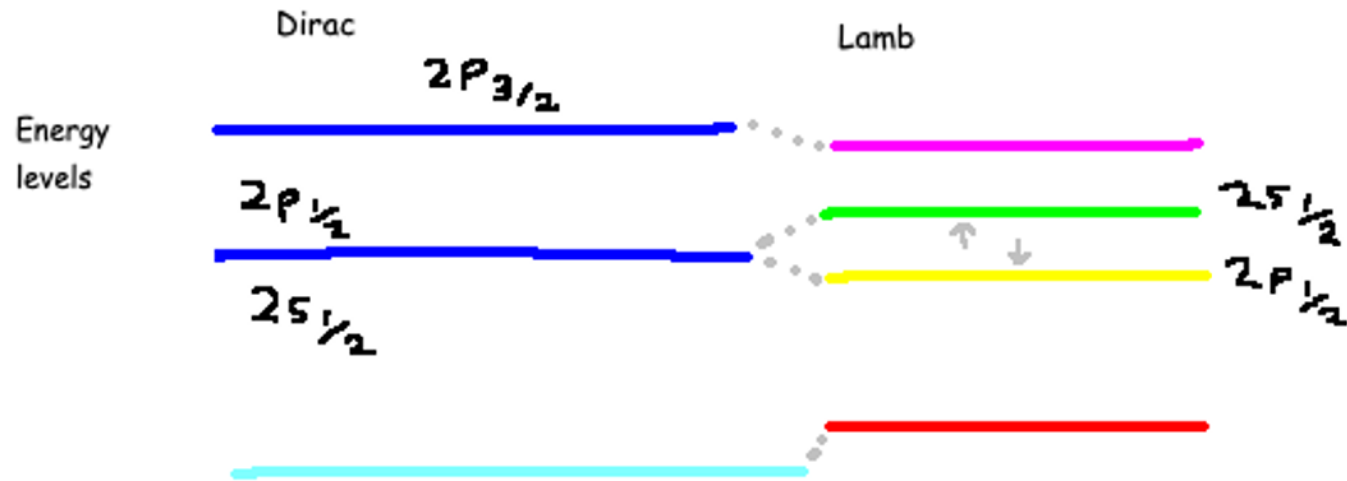
$$\Delta E = -\frac{\alpha^2 E_n}{n} \left(\frac{1}{j + \frac{1}{2}} - \frac{3}{4n} \right)$$

- Energy levels depend on
 - ① principal quantum number n
 - ② total angular momentum j

Precision determination of R_{∞} is important for any theoretical prediction of atomic spectroscopy

Spectroscopy and quantum field theory

- Important observable – Lamb shift

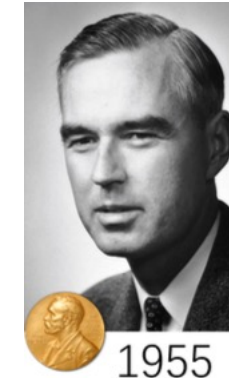


Dirac theory predicts that $2P_{1/2}$ and $2S_{1/2}$ states are degenerate

1947, Lamb discovered the nondegeneracy



Lamb shift



1955

- QED - Lamb shift mainly originates from quantum fluctuation of EM fields (VP + electron self energy)

Theory : 1057832.3(3) kHz [PRA 93 (2016) 022513]

Experiment : 1057829.8(3.2) kHz [Science 365 (2019) 6457]

- Consistency between theory and experiment
 - ➡ Lay the foundation of QED
- High-precision measurement of spectroscopy
 - ➡ Provide information of proton's structure



Tomonaga



Schwinger

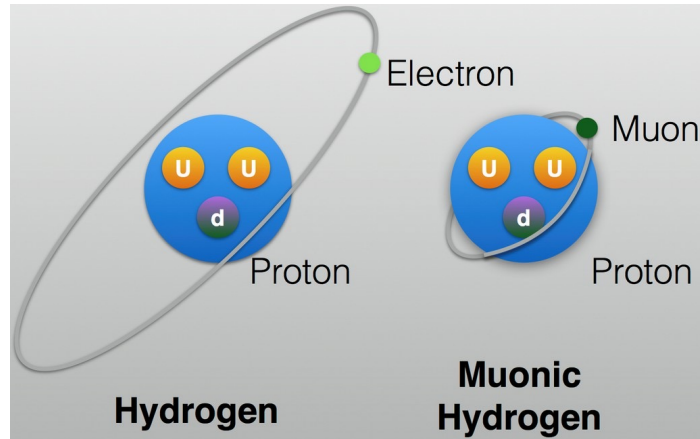


Feynman



1965

Muonic hydrogen



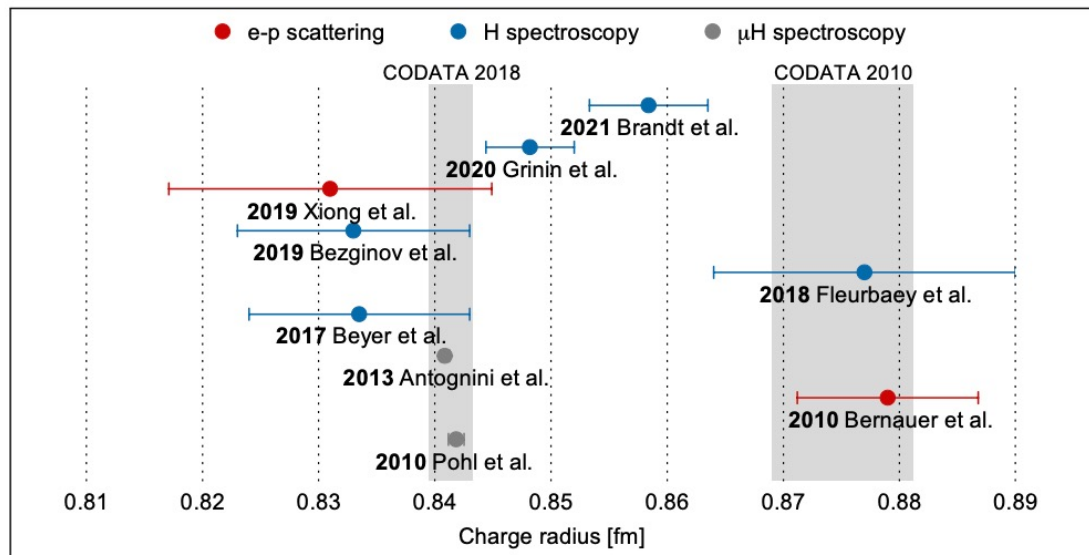
➤ 2010, proton charge radius from μH

【Nature 466 (2010) 213】

- Precision 10 times better than before
- 4% smaller radius

$>5\sigma$ deviation \rightarrow Proton size puzzle

- Muon mass is about 200 times of electron
- Bohr radius for μH is 200 times smaller than H



New experimental progress

- Still some discrepancies
- Consistently shrink the proton size



Puzzle possibly originates from experiments

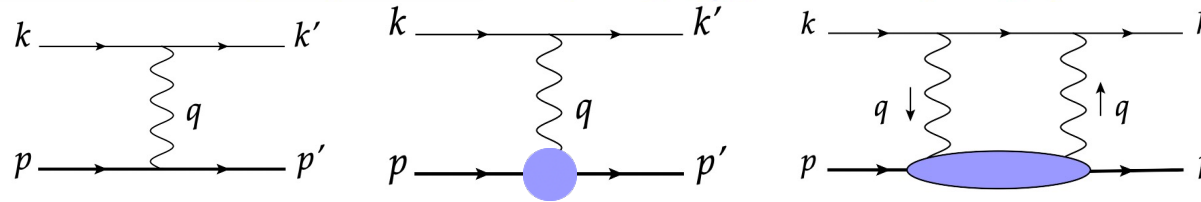
However, as a fundamental quantity, the size of proton charge radius plays an important role in the theoretical prediction in Rydberg const. and atomic spectroscopy

Various contributions to μH Lamb shift

Experiment Theory 【Science 339 (2013) 417】

$$E_{2P} - E_{2S} = \Delta E_{\text{QED}} + \Delta E_{\text{proton size}} + \Delta E_{\text{TPE}}$$

$$202370.6(2.3) = 206033.6(1.5) - 5227.5(1.0)\langle r_p^2 \rangle + 33.2(2.0) \mu\text{eV}$$



➤ Exp. vs Theory $\Rightarrow r_p = 0.84087(39) \text{ fm} \Rightarrow$ Proton size puzzle

➤ Largest theoretical uncertainty from **two-photon exchange (TPE)**

➤ Uncertainty for structure independent contribution is further reduced

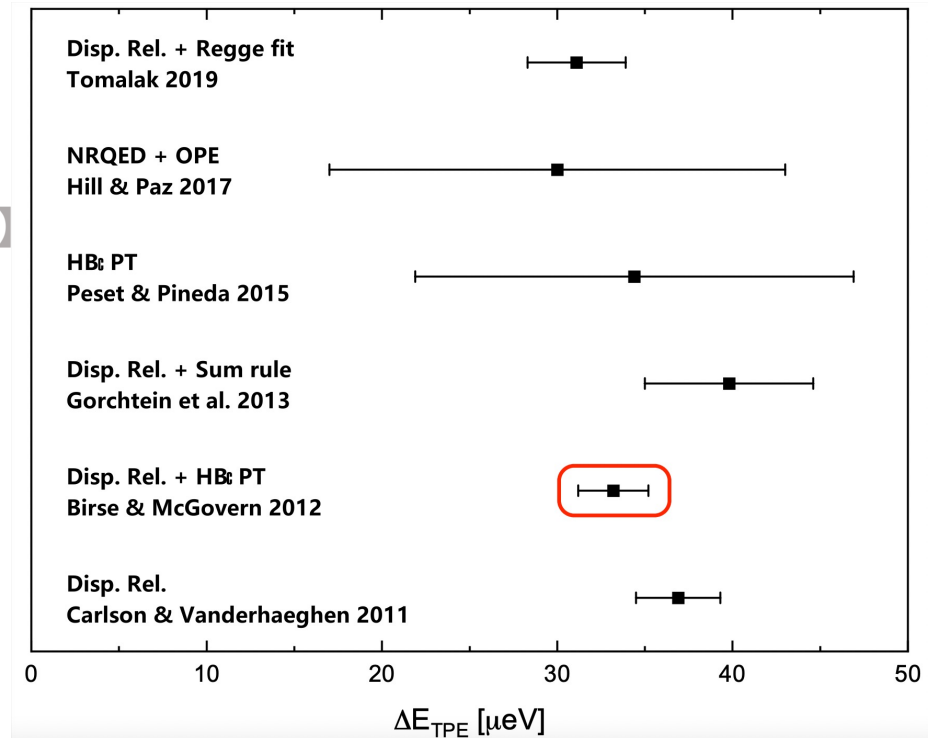
$$\Delta E_{\text{QED}} = 206034.7(0.3) \mu\text{eV} \quad \text{【Ann.Rev.Nucl.Part.Sci.72 (2022) 389】}$$

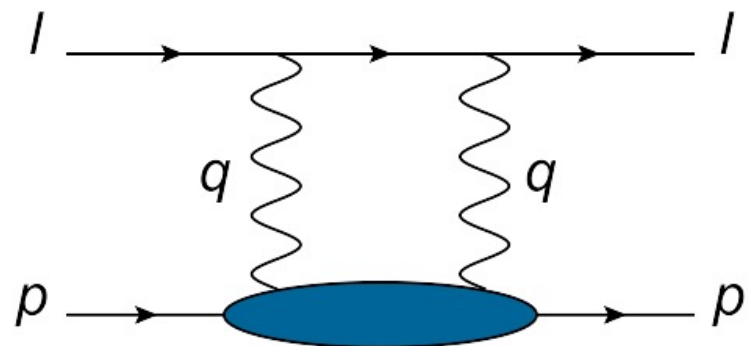
Upgrade of CREMA@PSI can reduce Exp. error by a factor of 5

Leaving TPE the important source for uncertainty!

➤ Theoretical prediction for TPE relies on data + models and ranges from 20 to 50 μeV

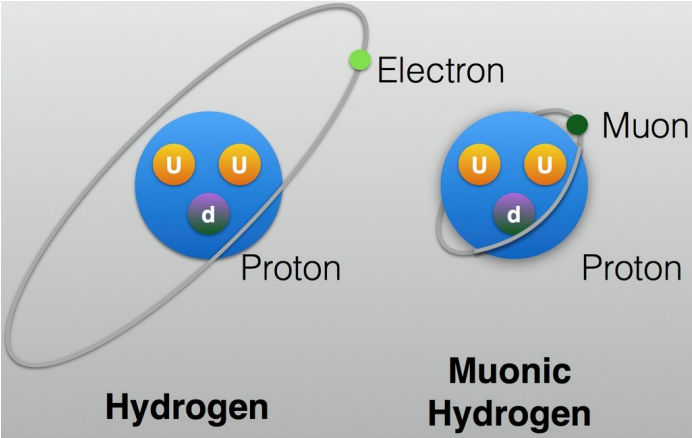
Our target: obtain TPE from first principles \Rightarrow Lattice QCD





Direct lattice QCD calculation

Challenges from TPE (1): IR divergence



➤ Binding energy of μH serves as a natural IR cutoff

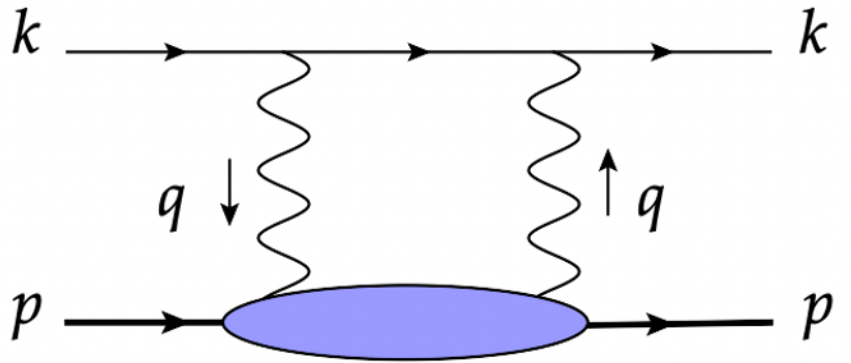


Bound-state QED



Proton treated as point-like particle
+ charge radius correction

No divergence, but rich structure information lost



➤ QCD+QED: complete information of proton structure

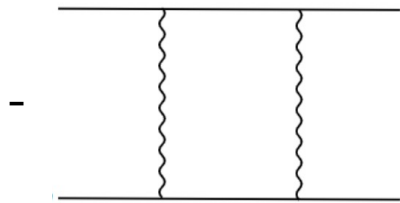
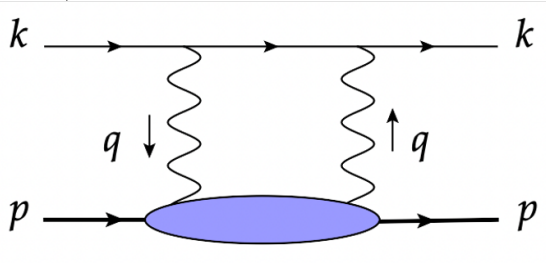


Loop integral sensitive to hadronic scale \rightarrow highly NP

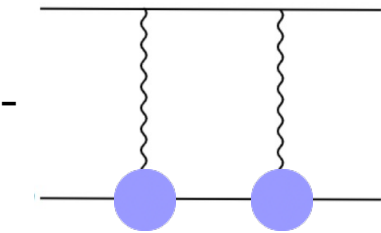


Bound lepton \rightarrow free lepton \rightarrow IR divergence

Solution: subtract the divergence

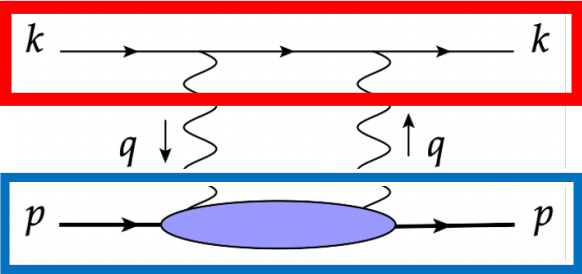


Point-like particle



Charge radius

Challenges from TPE (1): IR divergence



Leptonic part: $L_{\mu\nu}(q) \rightarrow$ Analytically known

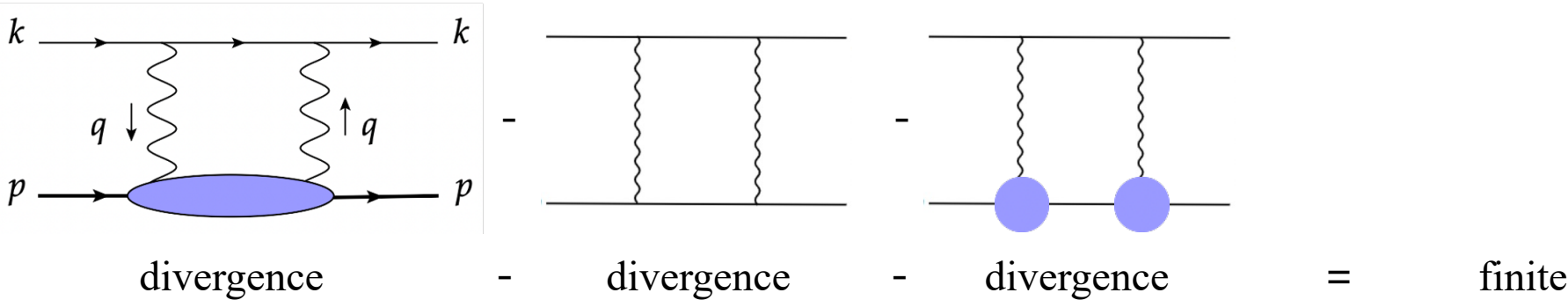
Hadronic part: $H_{\mu\nu}(q) \rightarrow$ Provided by LQCD
(statistical errors)

Loop integral

$$\Delta E^{\text{IR-}\infty} = \int \frac{d^4q}{(2\pi)^4} L_{\mu\nu}(q) H_{\mu\nu}(q)$$

$$= \int d^4x L_{\mu\nu}(x) H_{\mu\nu}(x)$$

IR subtraction



Key technical problem

Three diagrams contain diff. stat. errors ➡ How to maintain the error cancellation?

If signal cancels and error does not, then signal is completely hidden by error



Challenges from TPE (1): IR divergence

To solve IR divergence: infinite-volume reconstruction method 【X. Feng, L. Jin, PRD 100 (2019) 094509】

Basic idea: low-energy structure information is contained in the long-distance part of hadronic function

Use $H_{\mu\nu}(x)$ to reconstruct the quantities such as charge radius



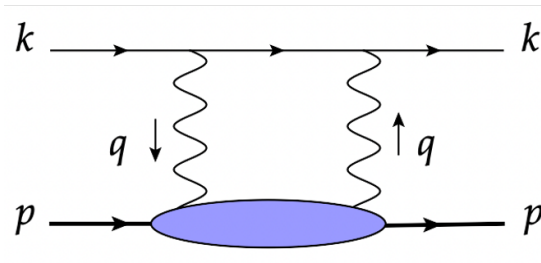
- Find the appropriate weight functions $L_{\mu\nu}^{\text{pt-like}}$ and $L_{\mu\nu}^{\text{radius}}$ for the subtraction terms, yielding



$$= \int d^4x L_{\mu\nu}^{\text{pt-like}}(x) H_{\mu\nu}(x)$$


$$= \int d^4x L_{\mu\nu}^{\text{radius}}(x) H_{\mu\nu}(x)$$

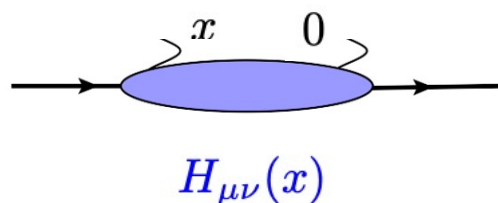
- Cancellation of IR divergence is rigorously fulfilled via the subtraction of weight functions



$$- \text{[pt-like diagram]} - \text{[radius diagram]} \Rightarrow L_{\mu\nu}^{\text{sub}} = L_{\mu\nu} - L_{\mu\nu}^{\text{pt-like}} - L_{\mu\nu}^{\text{radius}}$$

$$\Delta E^{\text{IR-finite}} = \int d^4x L_{\mu\nu}^{\text{sub}}(x) H_{\mu\nu}(x) \Rightarrow \text{Error decreases coherently as signal. IR divergence is solved cleanly!}$$

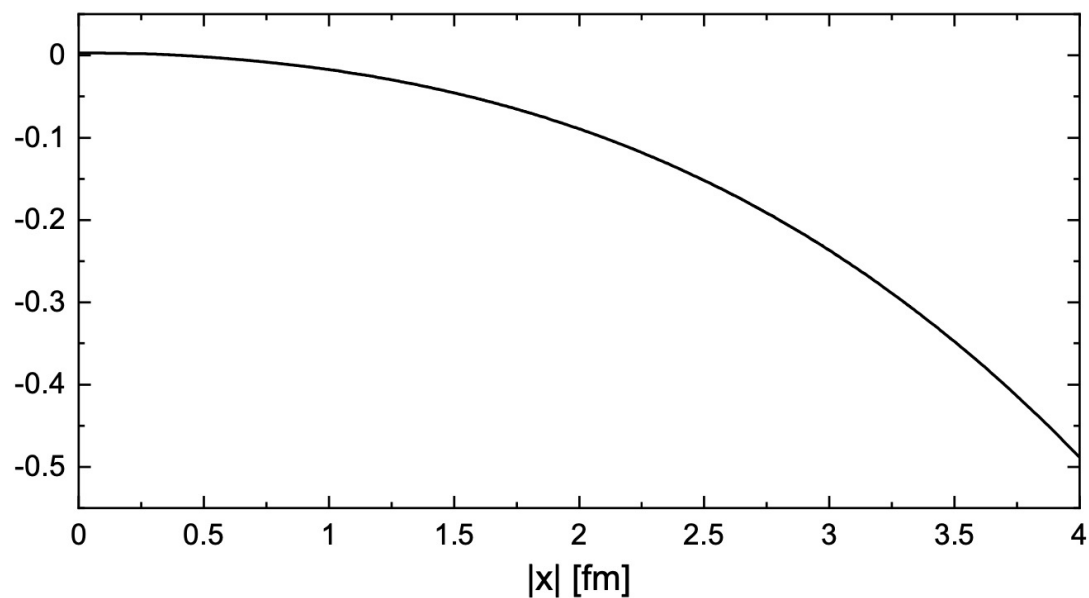
Challenges from TPE (2): Signal-to-noise problem



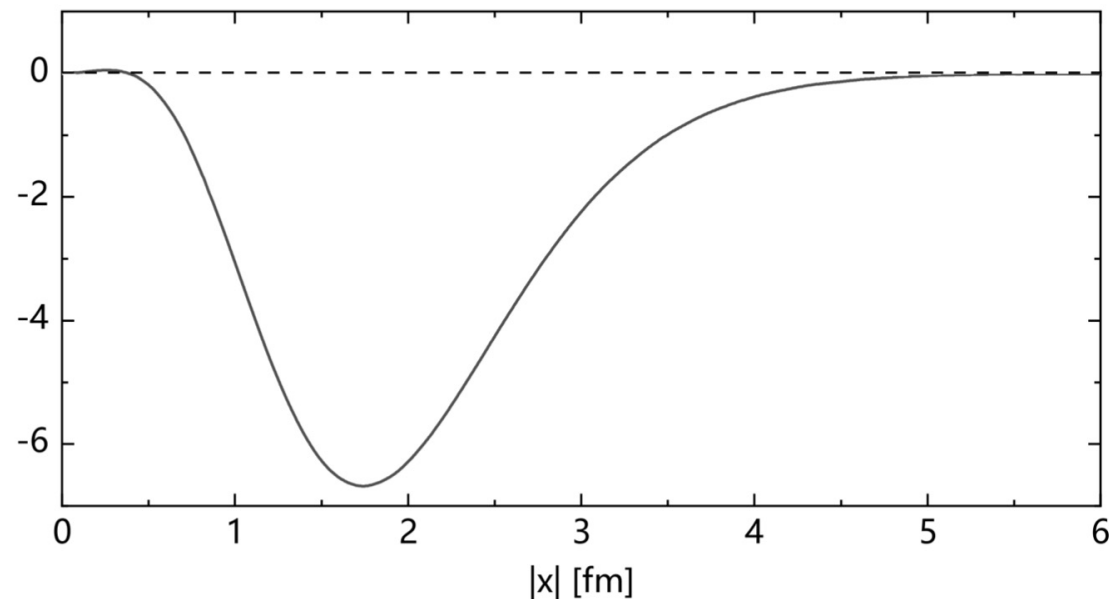
Property of lattice data:

As x increases, proton matrix element $H_{\mu\nu}(x)$ decreases as $e^{-M_p|x|}$

However, error decreases as $e^{-\frac{3}{2}M_\pi|x|}$



Weight function $L_{\mu\nu}^{sub}(x)$ increases fast, as x increases



Model estimate: Combine leptonic and hadronic part

Conclusion: take x as large as 5 fm

to guarantee no information lost



Require a 10 fm lattice for simulation

Decrease of S/N ratio seems an inevitable problem

Challenges from TPE (2): Signal-to-noise problem

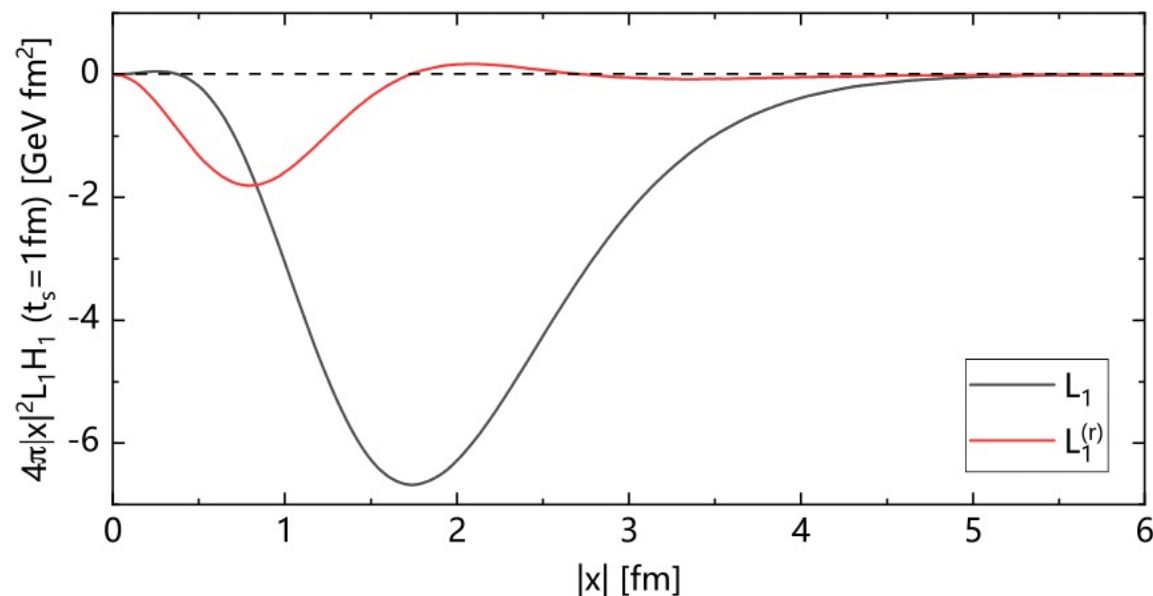
To solve S/N problem: optimized subtraction scheme 【Y. Fu, X. Feng, L. Jin, C. Lu, PRL 128 (2022) 172002】

Trick: $A = (A - B) + B$

Define the reduced weight function

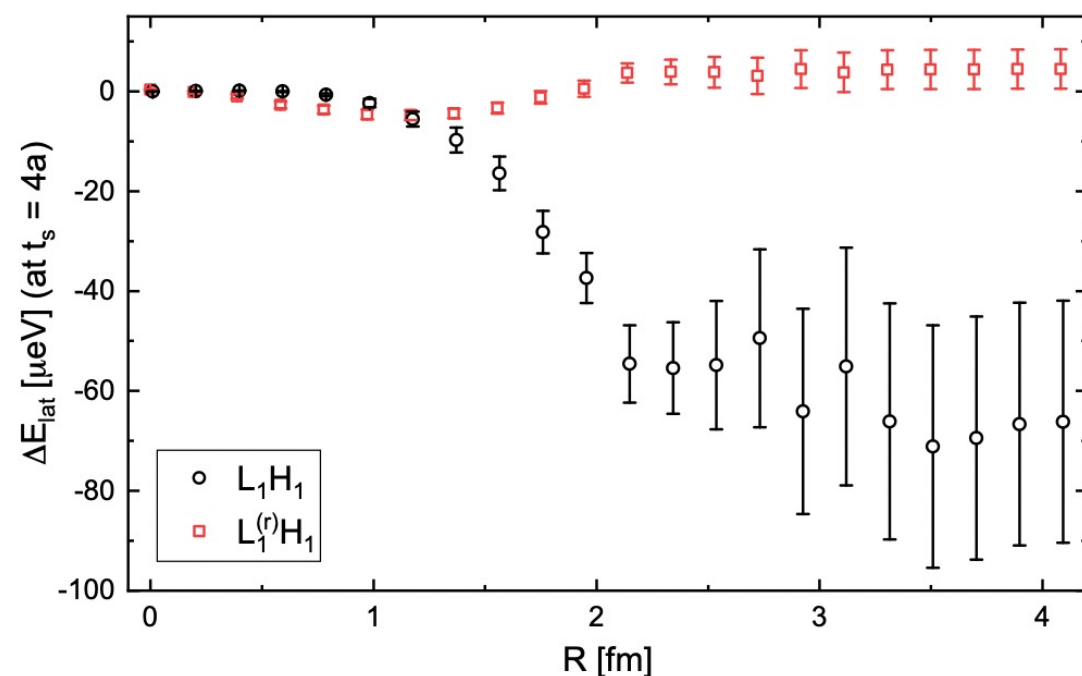
$$L^{(r)}(x) = L^{\text{sub}}(x) - c_0 L^{\text{pt-like}}(x) - c_r L^{\text{radius}}(x)$$

- Choose c_0, c_r to minimize $L^{(r)}(x)$ in the region of 1-3 fm
- Using $L^{(r)}(x)$, (A-B) part is illustrated by the red curve



- Total contribution is $\Delta E = \Delta E^{(r)} + c_0 + c_r \cdot \langle r_p^2 \rangle$

Use optimized subtraction scheme in realistic calculation



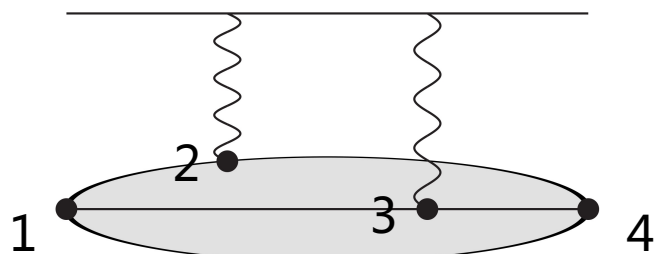
Integral within the range R:

using $L^{(r)}(x)$, error reduced by a factor of 6!

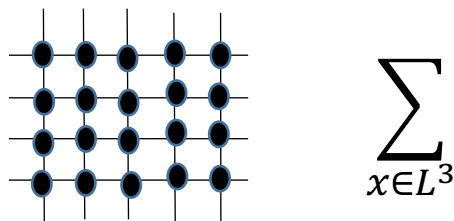
S/N problem is solved

Challenges from TPE (3): Computation of 4-point function

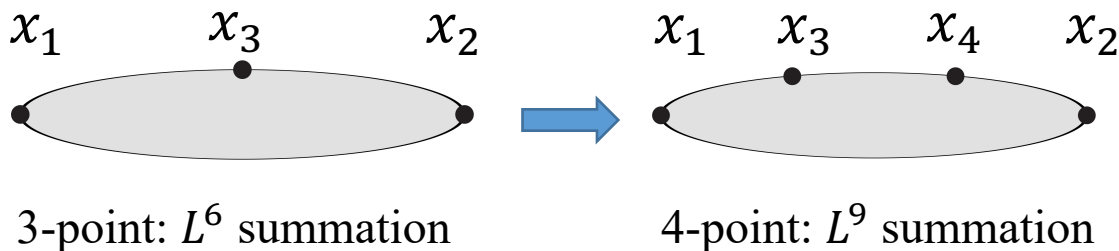
- TPE - hadronic part from a typical 4-point function



- Perform the volume summation for each point



- From 3-point to 4-point function

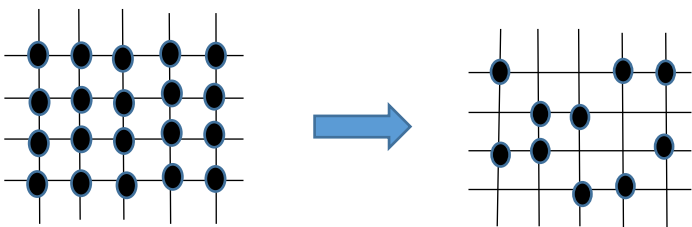


Increasing each point, computational cost increases by 10^4 - 10^5 times!
Cannot be solved by increasing resources ...

Solution : Field sparsening method

【Y. Li, S. Xia, X. Feng, L. Jin, C. Liu, PRD 103 (2021) 014514】

【W. Detmold, D. Murphy, et. al. PRD 104 (2021) 034502】



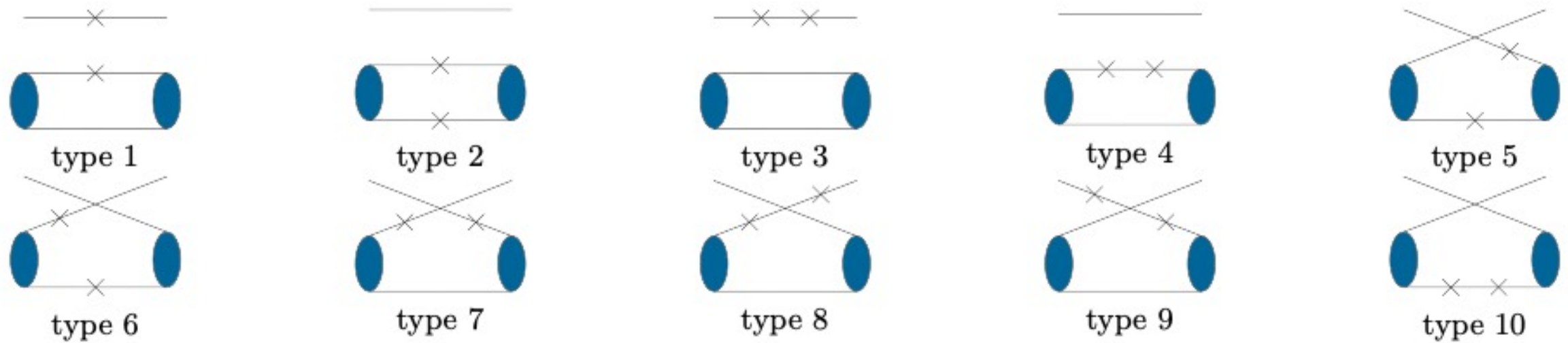
- Less summation points may lead to lower precision
- It is not the case because of high correlation in lattice data
➡ $\sim 10^3$ times less points yields similar precision
- Used for diff. physical system to confirm the universality

Utilize field sparsening method

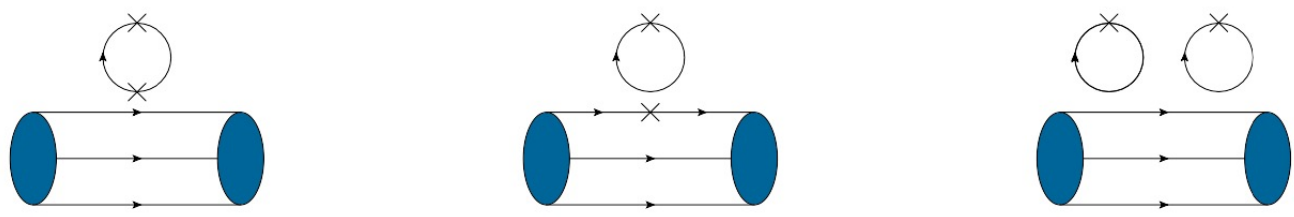
- Reduce the computational cost by a factor of $\sim 10^3$ with almost no loss of precision!

Challenges from TPE (3): Computation of 4-point function

- Complicated quark field contraction for nucleon 4-point function – 10 types of connected diagrams

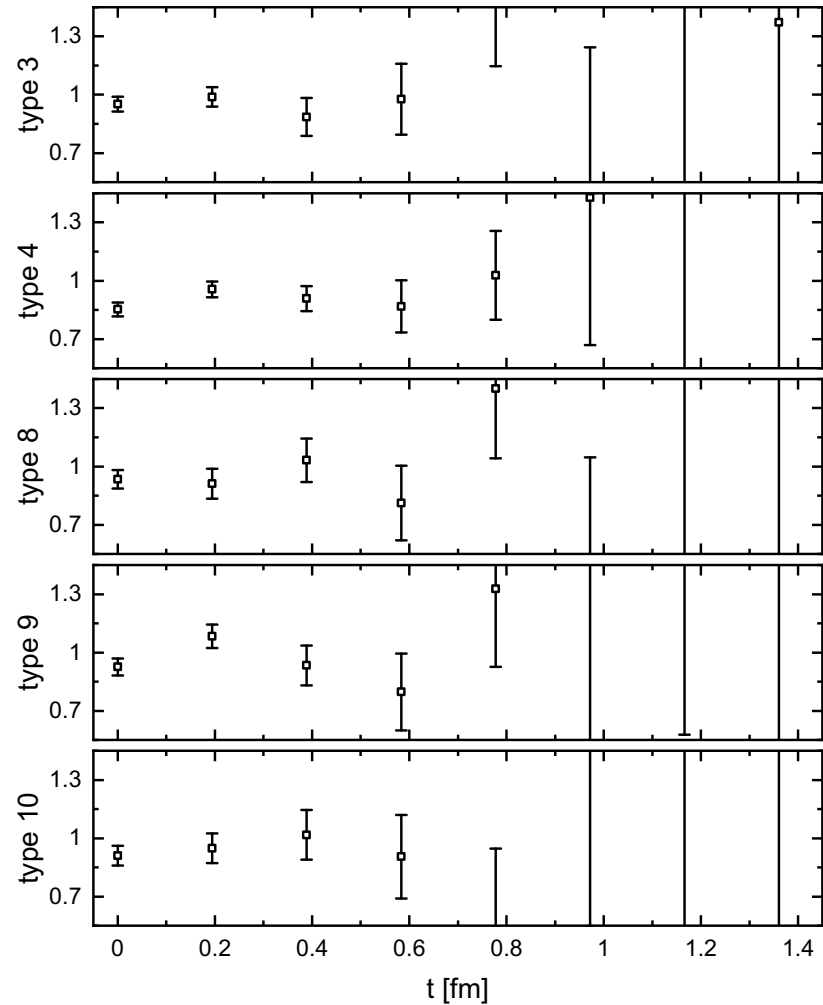


- There are also disconnected diagrams – notorious for high cost and bad S/N ratio

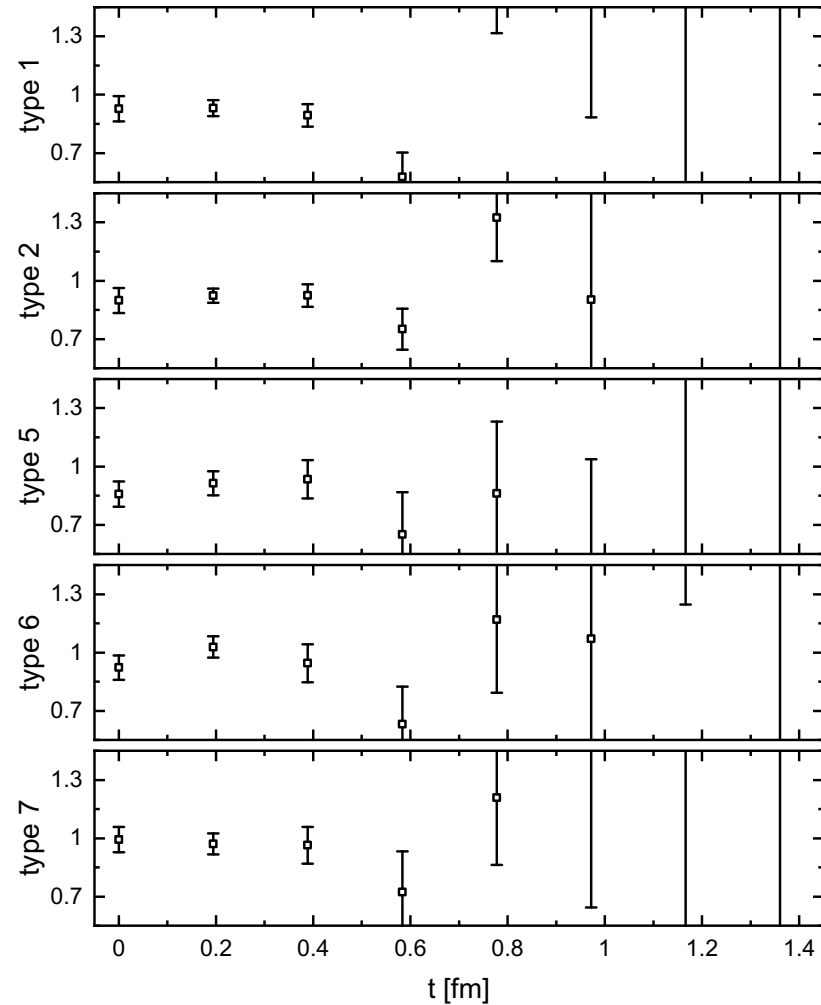


Our calculation contains both connected and the main disconnected diagrams

Challenges from TPE (3): Computation of 4-point function



Two currents inserted in one quark line



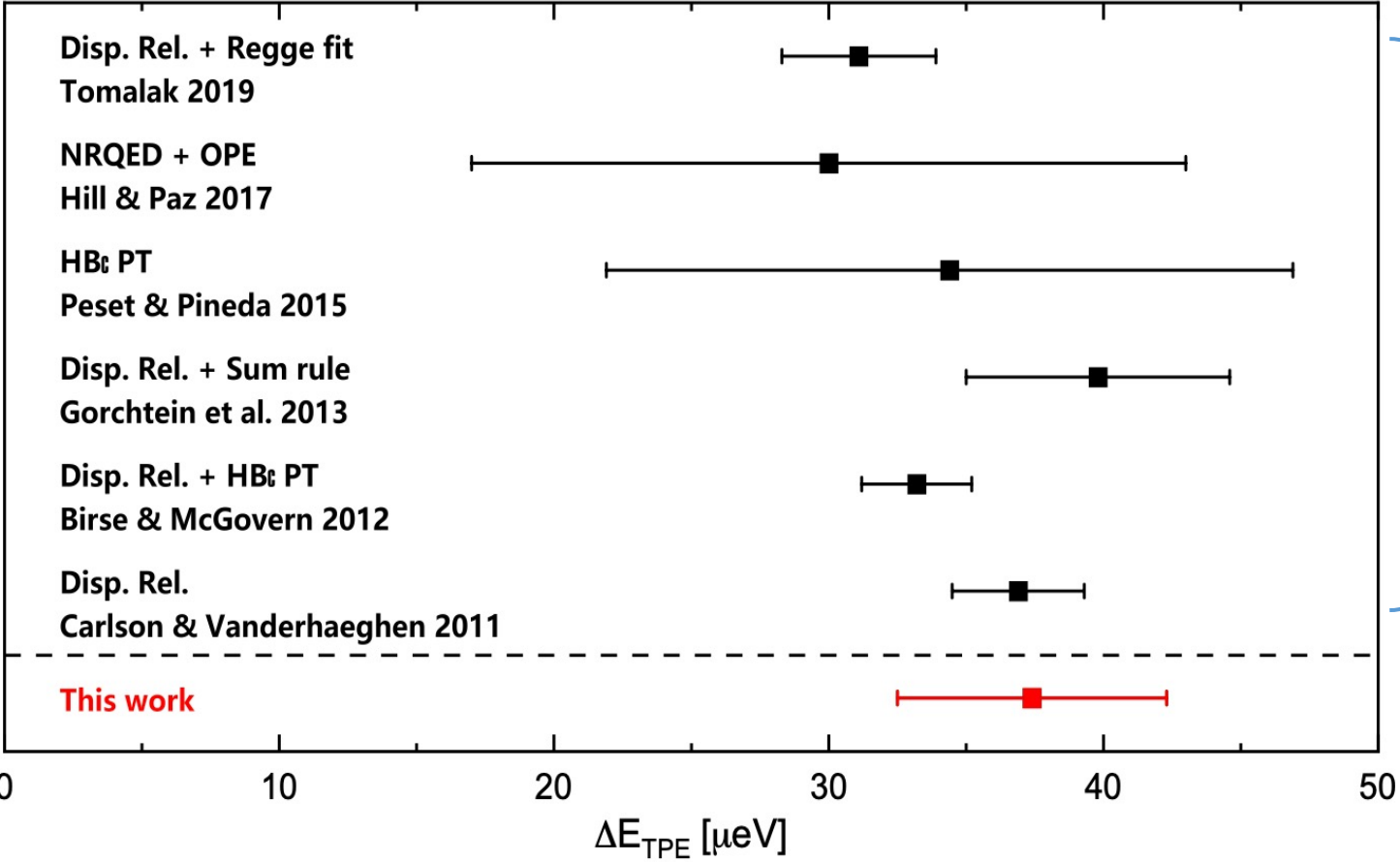
Two currents inserted in two quark lines

Using the conditions such as charge conservation to verify the contraction code

First lattice calculation

➤ Gauge ensemble used – nearly physical pion mass

Ensemble	m_π [MeV]	L/a	T/a	a [fm]	N_{conf}
24D	142	24	64	0.1943(8)	131



- Dispersive analysis
- ranges from 20 to 50 μeV
- Lattice results
- desirable to improve precision

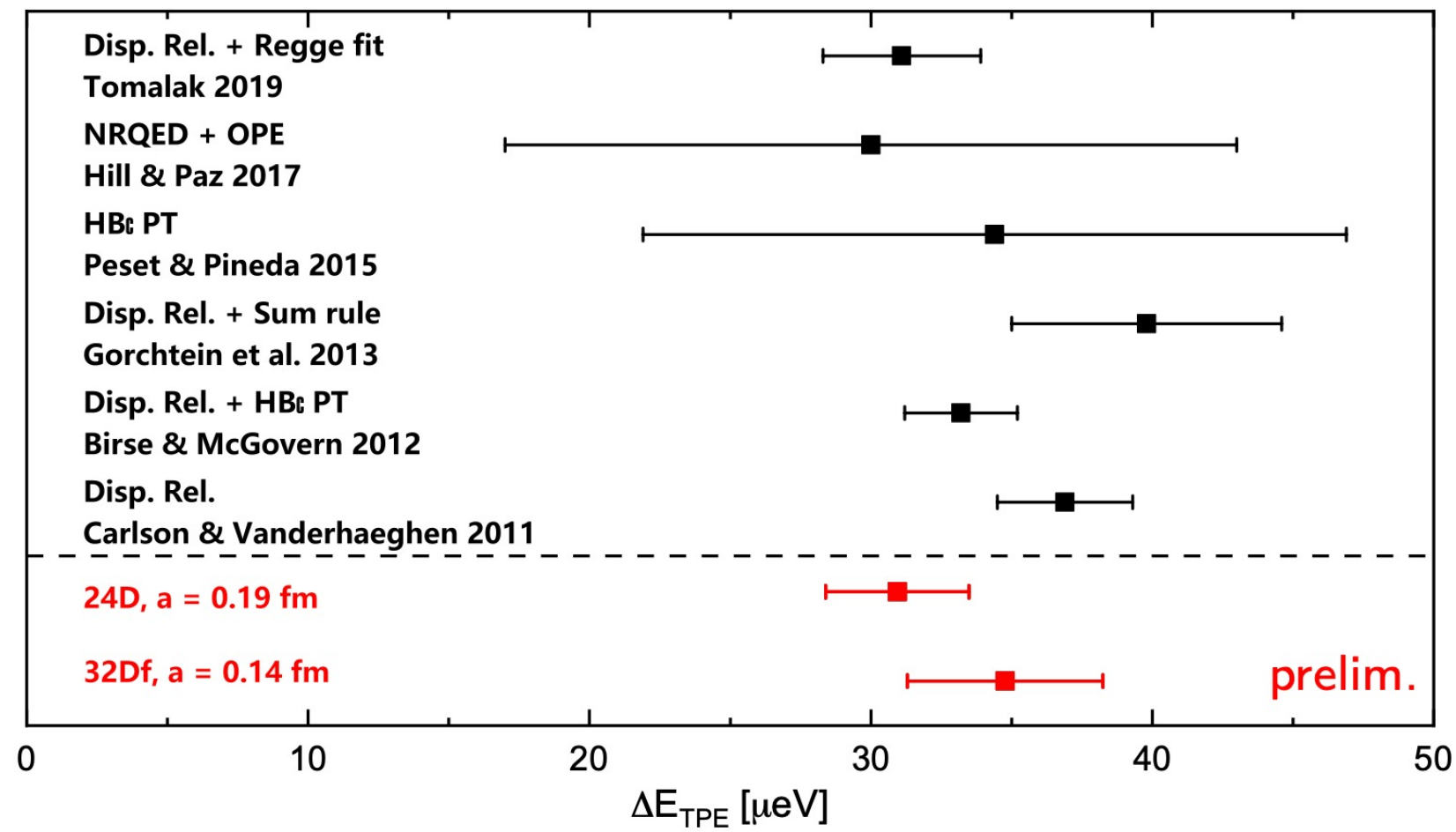
Y. Fu, XF, L. Jin, C. Lu, PRL 128 (2022) 172002

Updated results

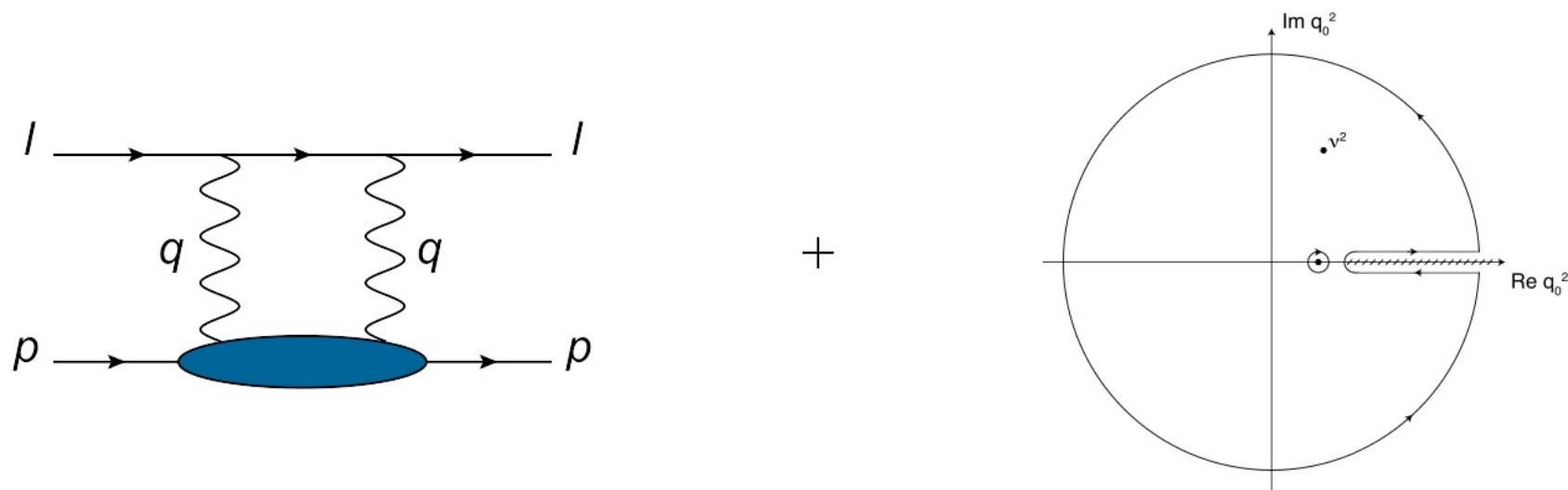
➤ Second ensemble

finer lattice spacing, same pion mass and volume

Ens.	m_π [MeV]	L/a	T/a	L	a [fm]	N_{conf}
24D	142	24	64	4.6	0.194	207
32Df	142	32	64	4.6	0.143	82



More statistics & gauge ensembles are on-going!



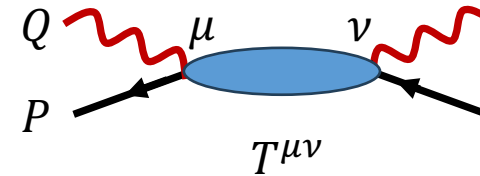
Joint lattice QCD & dispersive analysis

Dispersion relation

- External nucleon has zero three momentum $P = (iM, \vec{0})$

➡ two kinematics

$$Q^2, \nu = \frac{P \cdot Q}{M} = iQ_0$$



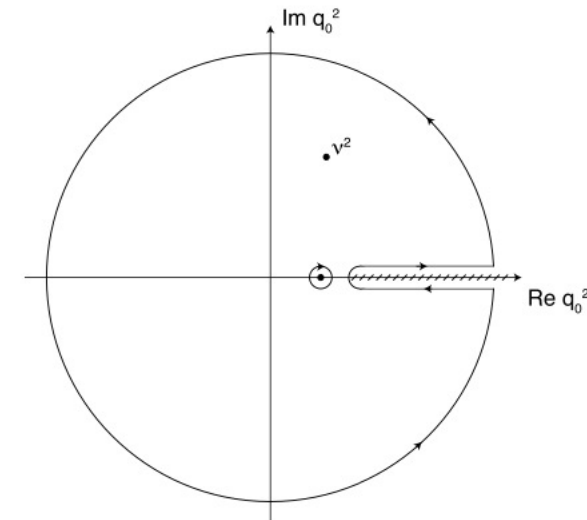
- Spin-averaged Compton tensor

$$T^{\mu\nu} = \frac{1}{8\pi M} \int d^4x e^{iQx} \langle N(\mathbf{P}) | T[J^\mu(\vec{x}, t) J^\nu(0)] | N(\mathbf{P}) \rangle = K_1^{\mu\nu} T_1(\nu, Q^2) + K_2^{\mu\nu} T_2(\nu, Q^2)$$

- $K_{1,2}^{\mu\nu}$ are two Lorentz kinematic factors
- $T_{1,2}(\nu, Q^2)$ are non-perturbative Lorentz scalar amplitude
- Dispersion relation: construct $T_{1,2}$ using experimental data as input

$$T_i(\nu, Q^2) = \int_{\nu_{el}^2}^{\infty} \frac{d\nu'^2}{\pi} \frac{\text{Im} T_i(\nu', Q^2)}{\nu'^2 - \nu^2}$$

- $\text{Im} T_i(\nu', Q^2)$ are from e-p scattering data
- It requires sufficiently fast convergence at large ν'^2



Bottle neck in dispersive analysis

- UV divergence requires the once-subtracted dispersion relation for T_1

$$T_1(\nu, Q^2) - T_1(\nu_0, Q^2) = \int_{\nu_{\text{el}}^2}^{\infty} \frac{d\nu'^2}{\pi} \left[\frac{1}{\nu'^2 - \nu^2} - \frac{1}{\nu'^2 - \nu_0^2} \right] \text{Im } T_1(\nu', Q^2)$$

$T_1(\nu_0, Q^2)$ at reference point $\nu_0 = 0$ is called as **subtraction function** ➡ It depends on **model assumption**

- F. Hagelstein & V. Pascalutsa propose a different subtraction point for lattice QCD calculation 【NPA 1016 (2021) 122323】

Subtraction at $\nu_0 = iQ$ rather than $\nu_0 = 0$ ➡ Main non-Born contribution contained in the subtraction function

- In our lattice calculation, we try with various subtraction point at $\nu_0 = i\xi Q$

$$T_1(i\xi Q, Q^2) = \frac{1}{2} \left[\frac{\xi^2}{1 - \xi^2} (T^{00} - T_{\text{GS}}^{00}) - \sum_i (T^{ii} - T_{\text{GS}}^{ii}) \right] + \text{known form factor}$$

- It requires the subtraction of the ground-state contribution, thus very noisy!
- When $\xi \rightarrow 1$, we analytically demonstrate that the expression can be significantly simplified

$$T_1(iQ, Q^2) = -\frac{1}{3} \sum_i T^{ii} \quad \text{No subtraction of ground state is required!}$$

How well lattice QCD compute the subtraction function

- UV divergence requires the once-subtracted dispersion relation for T_1

$$T_1(\nu, Q^2) - T_1(iQ, Q^2) = \int_{\nu_{\text{el}}^2}^{\infty} \frac{d\nu'^2}{\pi} \left[\frac{1}{\nu'^2 - \nu^2} - \frac{1}{\nu'^2 + Q^2} \right] \text{Im } T_1(\nu', Q^2)$$

Input from lattice QCD

Input from exp. measurement

- Question: how well lattice QCD can determine $T_1(iQ, Q^2)$
- When $Q \rightarrow 0$, the subtraction function can be related to the proton electric polarizability

κ : anomalous magnetic moment

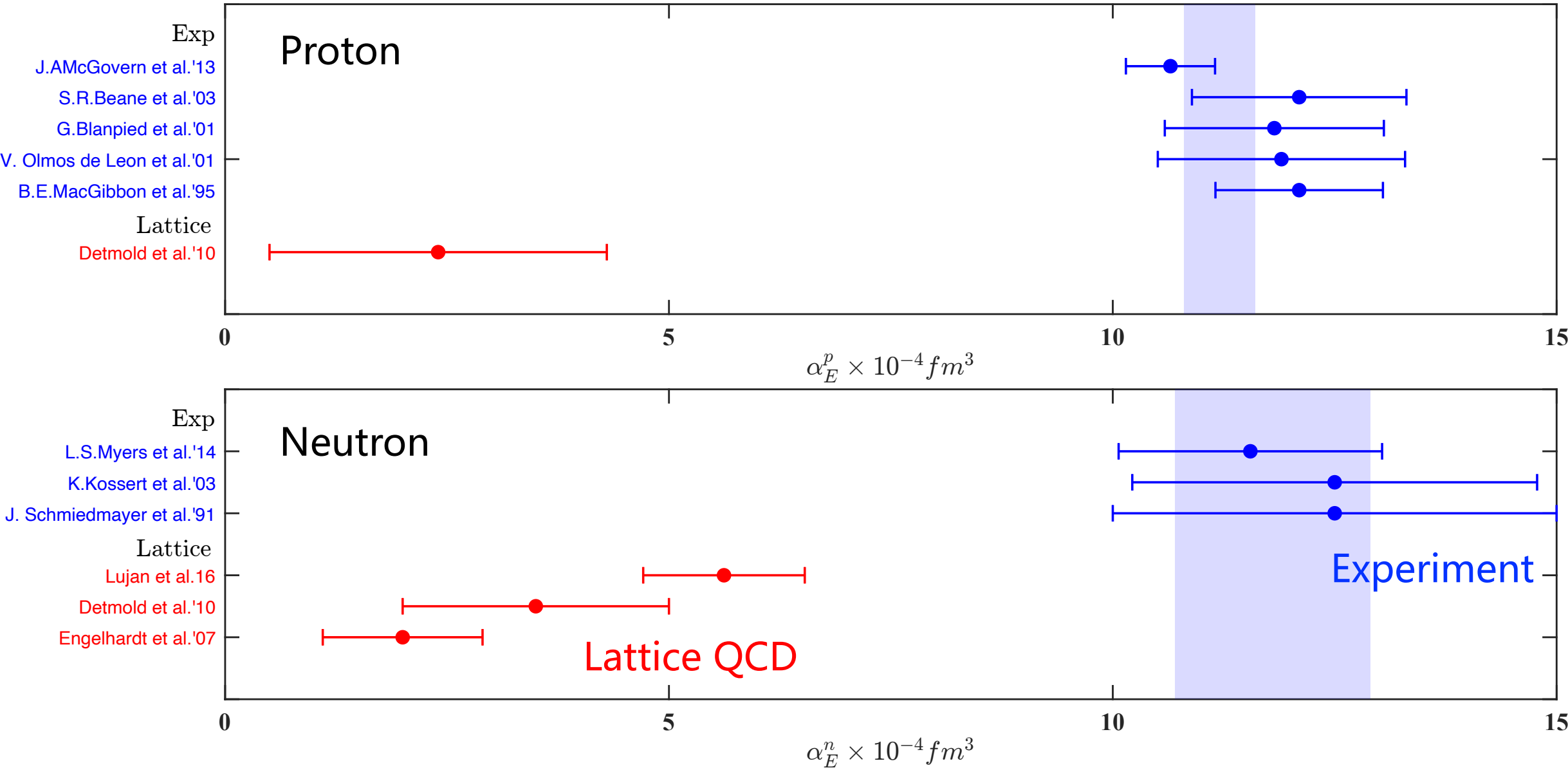
$\langle r_p^2 \rangle$: squared charge radius

$$\lim_{Q \rightarrow 0} T_1(iQ, Q^2) = \alpha_E - \frac{\alpha_{\text{em}}}{M} \left(\frac{1 + \kappa^2}{4M^2} + \frac{\langle r_p^2 \rangle}{3} \right)$$

α_E : polarizability

- Question: how well lattice QCD can determine α_E ?

Determination of electric polarizabilities



Determination of electric polarizabilities

➤ What is the primary source of discrepancy between lattice QCD and other studies?

① Lattice calculations are performed at unphysical pion masses, ranging from 227 - 759 MeV



Unphysical quark mass effects

② Background field technique is used, which converts 4pt function to 2pt function using Feynman-Hellman theorem



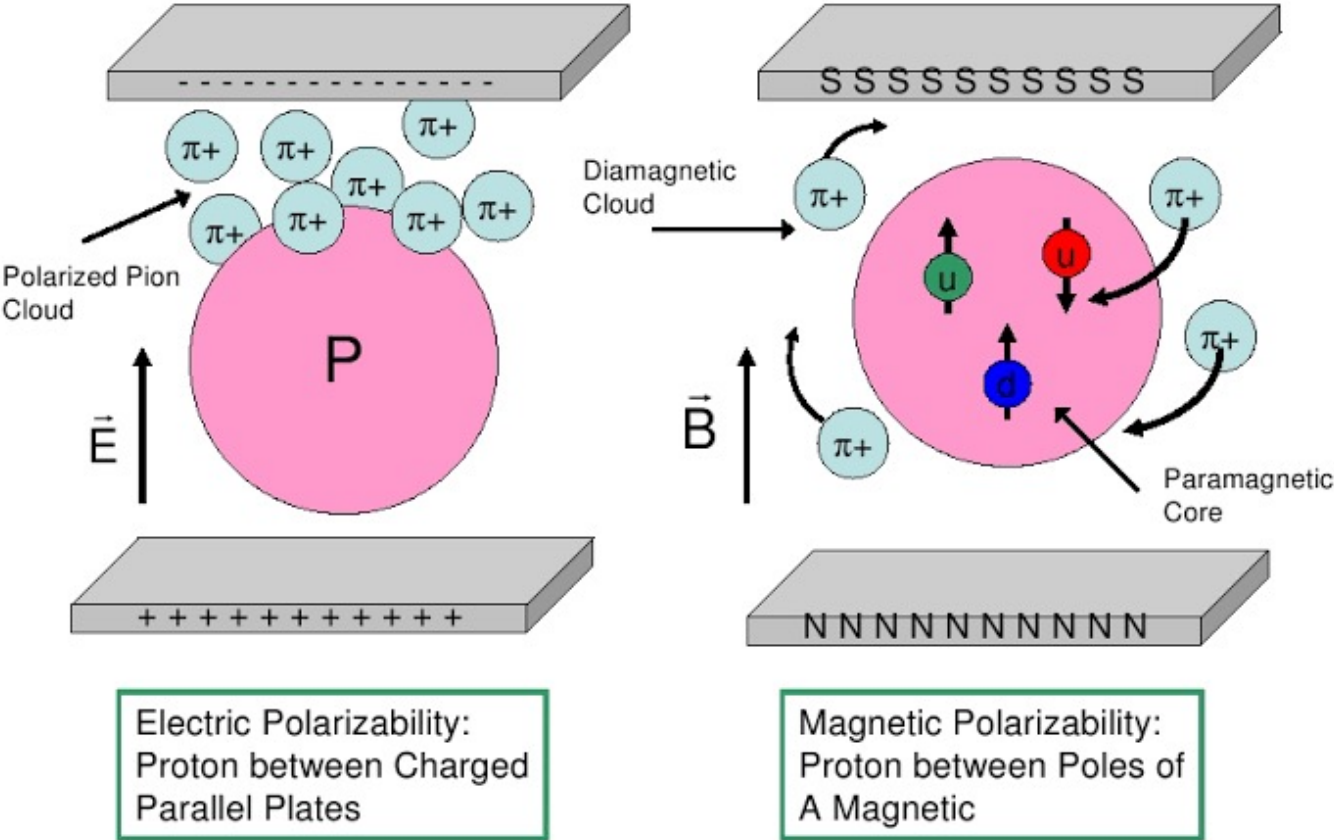
Hard to explore intermediate-state contributions and control systematics



Perform calculation at physical pion mass, using 4pt function

Why physical pion mass is important

➤ Pion cloud in nucleon polarizabilities



➤ Use two DWF ensembles @ physical π mass

Ensembles	m_π [MeV]	L/a	T/a	a[fm]	N_{conf}
24D	142.6(3)	24	64	0.1929	207
32Dfine	143.6(9)	32	64	0.1432	82

➤ LO in χ_{PT} :

$$\alpha_E = \frac{5}{96} \left(\frac{g_A}{f_\pi} \right)^2 \frac{\alpha_{em}}{m_\pi}$$

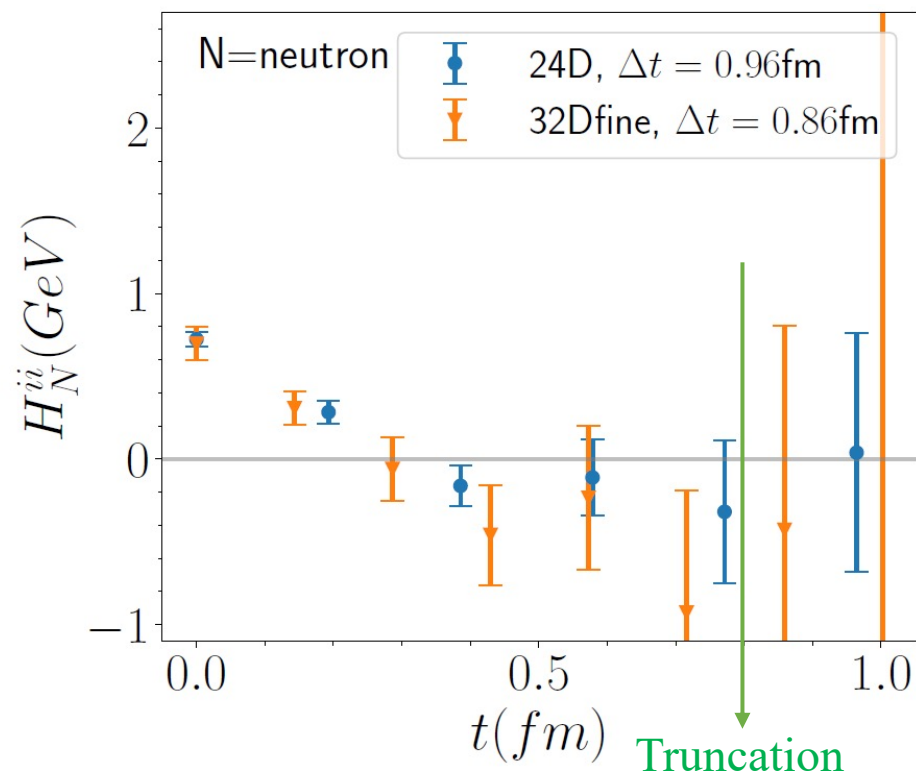
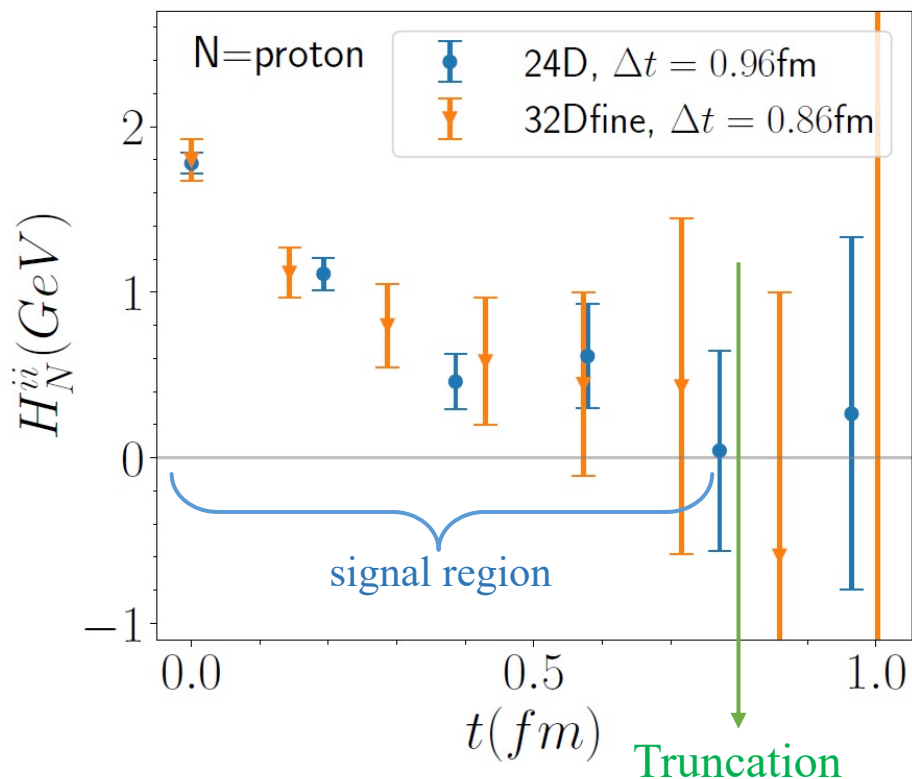
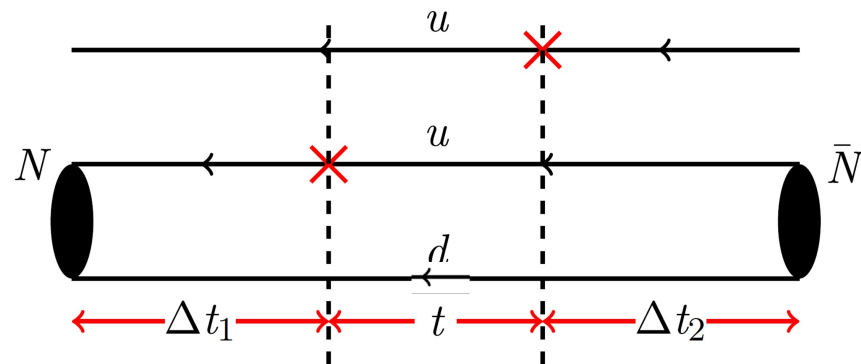
V. Bernard et al., Phys. Rev. Lett. 67 (1991) 1515



α_E is inversely proportional to pion mass

Signal of hadronic function

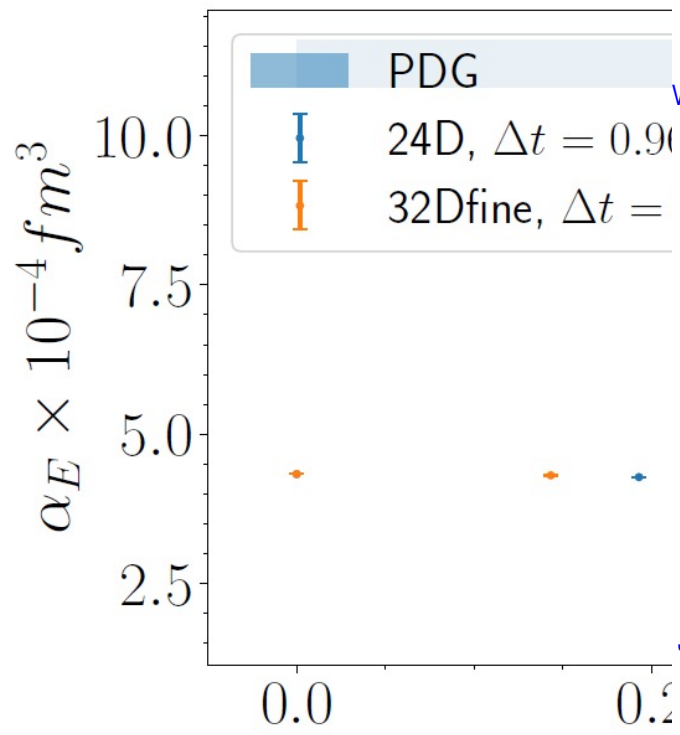
$$H_N^{ii}(t) = \sum_{\vec{x}} \langle N | T[J^i(\vec{x}, t) J^i(0)] | N \rangle = \sum_k \langle p | J^i(0) | k \rangle e^{-(E_k - M)t} \langle k | J^i(0) | p \rangle$$



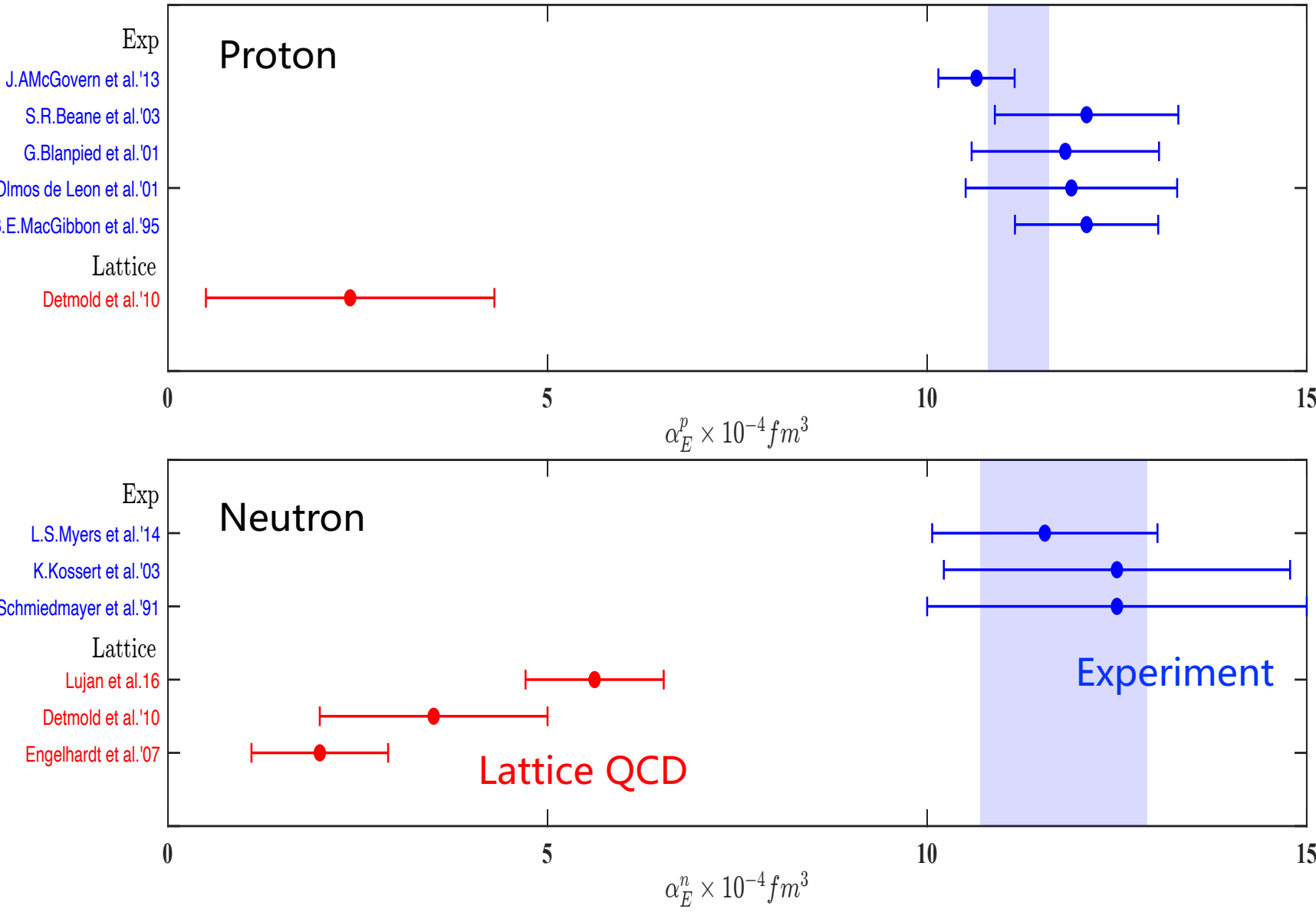
$$\Delta t = \Delta t_1 + \Delta t_2 = \begin{cases} 0.96 \text{ fm (24D)} \\ 0.86 \text{ fm (32Dfine)} \end{cases}, \text{ truncation at } t_0 = \begin{cases} 0.77 \text{ fm (24D)} \\ 0.72 \text{ fm (32Dfine)} \end{cases} \quad \Rightarrow \quad \text{In total, } \Delta t_1 + \Delta t_2 + t_0 \sim 1.6-1.8 \text{ fm}$$

Polarizability α_E from our calculation

Polarizability extraction

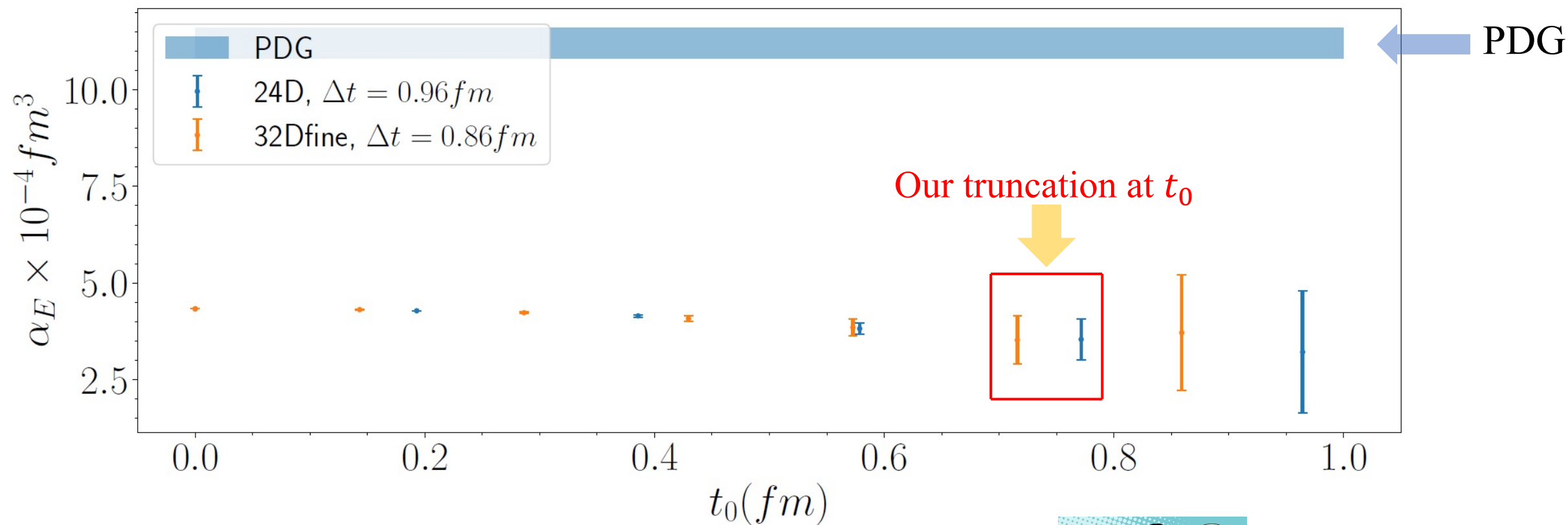


However, lattice results are



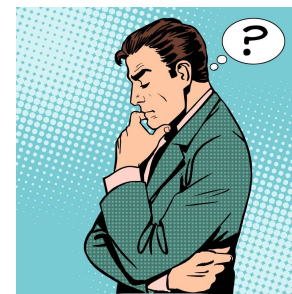
Polarizability α_E from our calculation

Polarizability extraction $\alpha_E = -\frac{\alpha_{em}}{12M} \int d^4x \, t^2 \langle N | T[J^i(x)J^i(0)] | N \rangle + \alpha_E^r$



However, lattice results are significantly below the PDG value.

Need new insight to turn the decent to the magic!

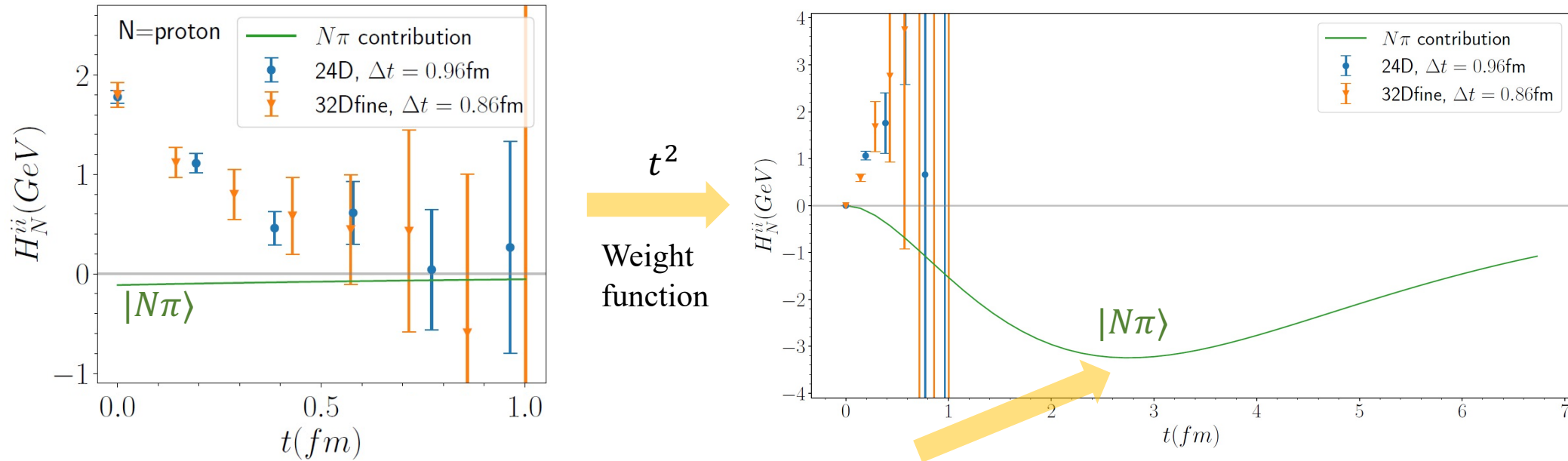


Nucleon polarizabilities and $N\pi$ scattering

Structure of hadronic function $\int d^4x \textcolor{red}{t}^2 H^{ii}(x, t) = \int dt \textcolor{red}{t}^2 \sum_k \langle p | J^i(0) | k \rangle e^{-(E_k - M)t} \langle k | J^i(0) | p \rangle$

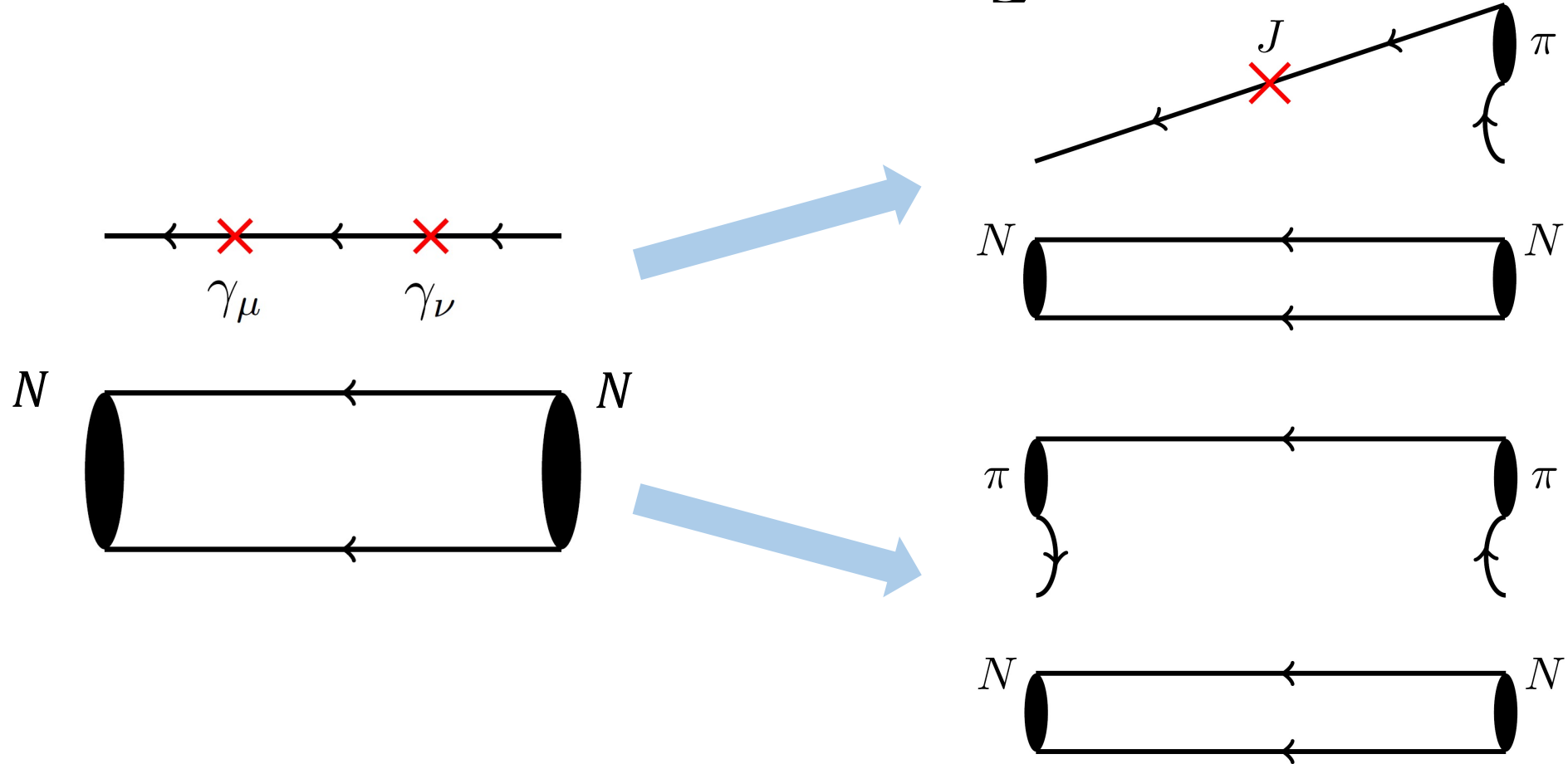
$$= 4 \sum_k \frac{\langle p | J^i(0) | k \rangle \langle k | J^i(0) | p \rangle}{(\textcolor{red}{E}_k - M)^3}$$

The dominant contribution is given by $|k\rangle = |N\pi\rangle$ states



$|N\pi\rangle$ states contribution exhibits a peak at $t = 2.8\text{ fm}$, far exceeding our truncation at $t_0 \approx 0.75\text{ fm}$
Must calculate $N\pi$ contribution directly!

Wick contraction of $N\pi$ rescattering



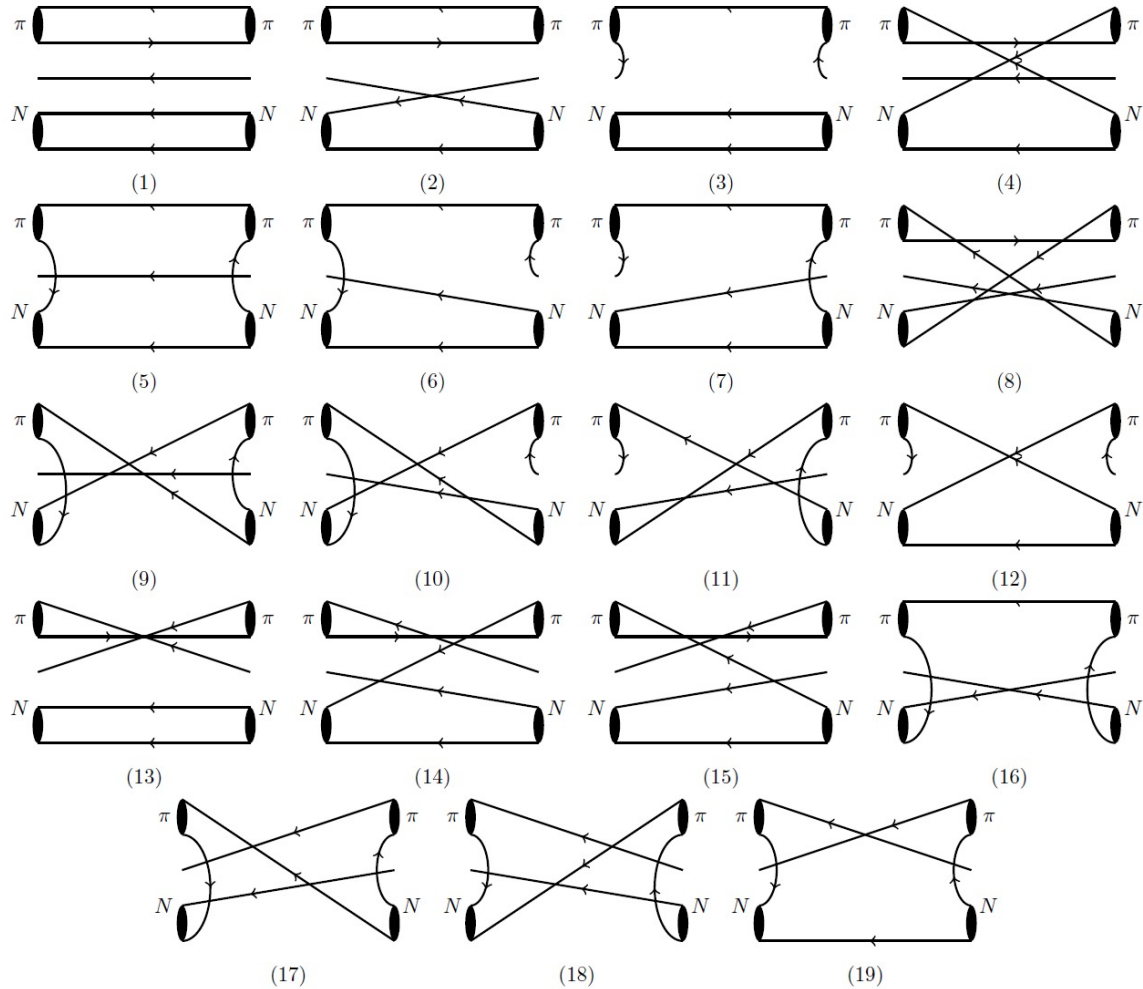
$$I = 1/2: O_{N\pi}^{I_3=+\frac{1}{2}} = O_p O_{\pi^0} - \sqrt{2} O_n O_{\pi^+}, O_{N\pi}^{I_3=-\frac{1}{2}} = \sqrt{2} O_n O_{\pi^0} - O_p O_{\pi^-}$$

$$I = 3/2: O_{N\pi}^{I_3=+\frac{1}{2}} = \sqrt{2} O_p O_{\pi^0} + O_n O_{\pi^+}, O_{N\pi}^{I_3=-\frac{1}{2}} = O_n O_{\pi^0} + \sqrt{2} O_p O_{\pi^-}$$

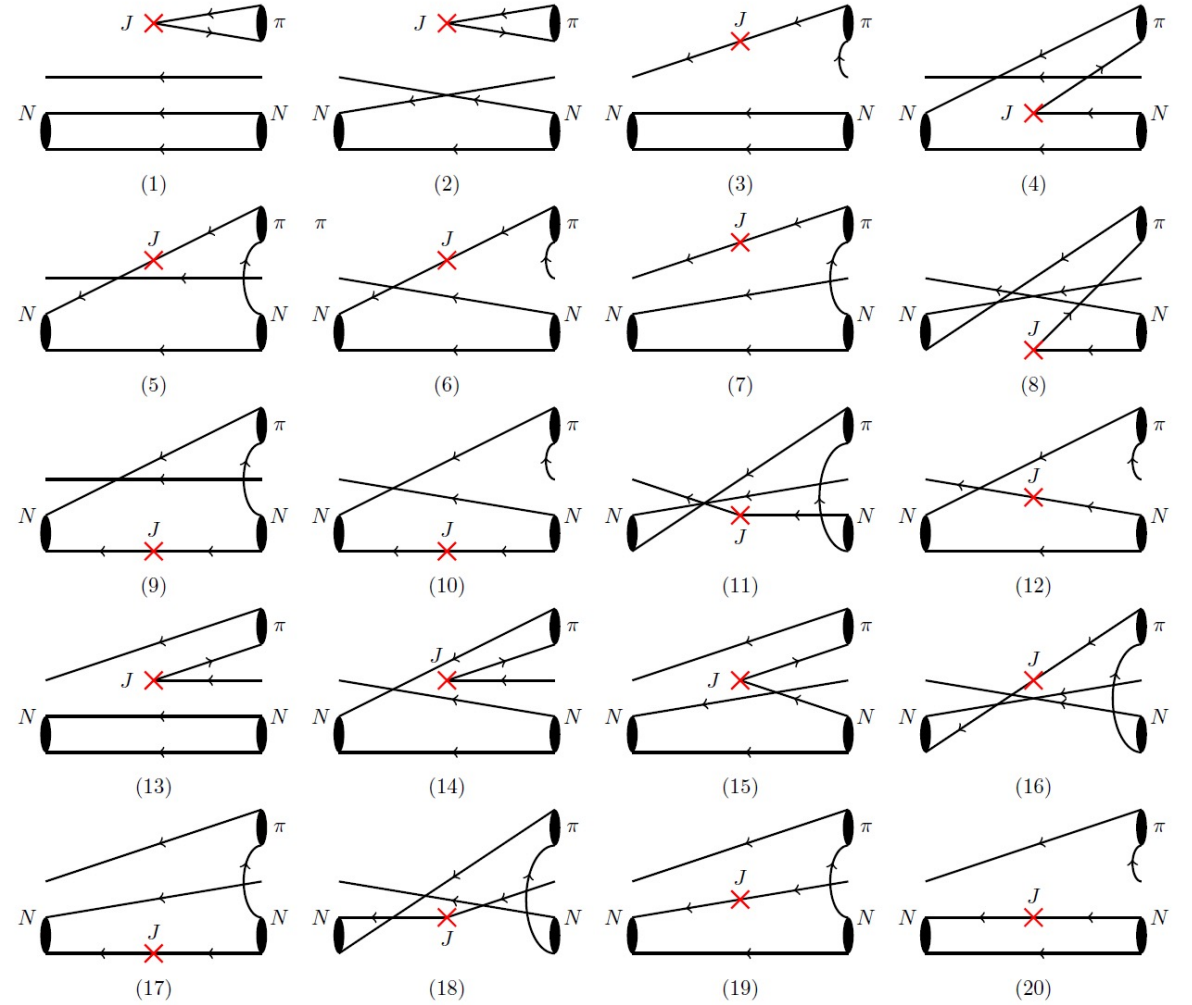
} Operators

Wick contraction of $N\pi$ Rescattering

➤ 19 diagrams for $N\pi$ rescattering



➤ 20 diagrams for $N + \gamma \rightarrow N\pi$



Results of $N\pi$ Scattering

➤ $N\pi$ scattering at $m_\pi=142$ MeV

$$R = \frac{C_2^{N\pi}(t)}{C_2^N(t)C_2^\pi(t)}$$

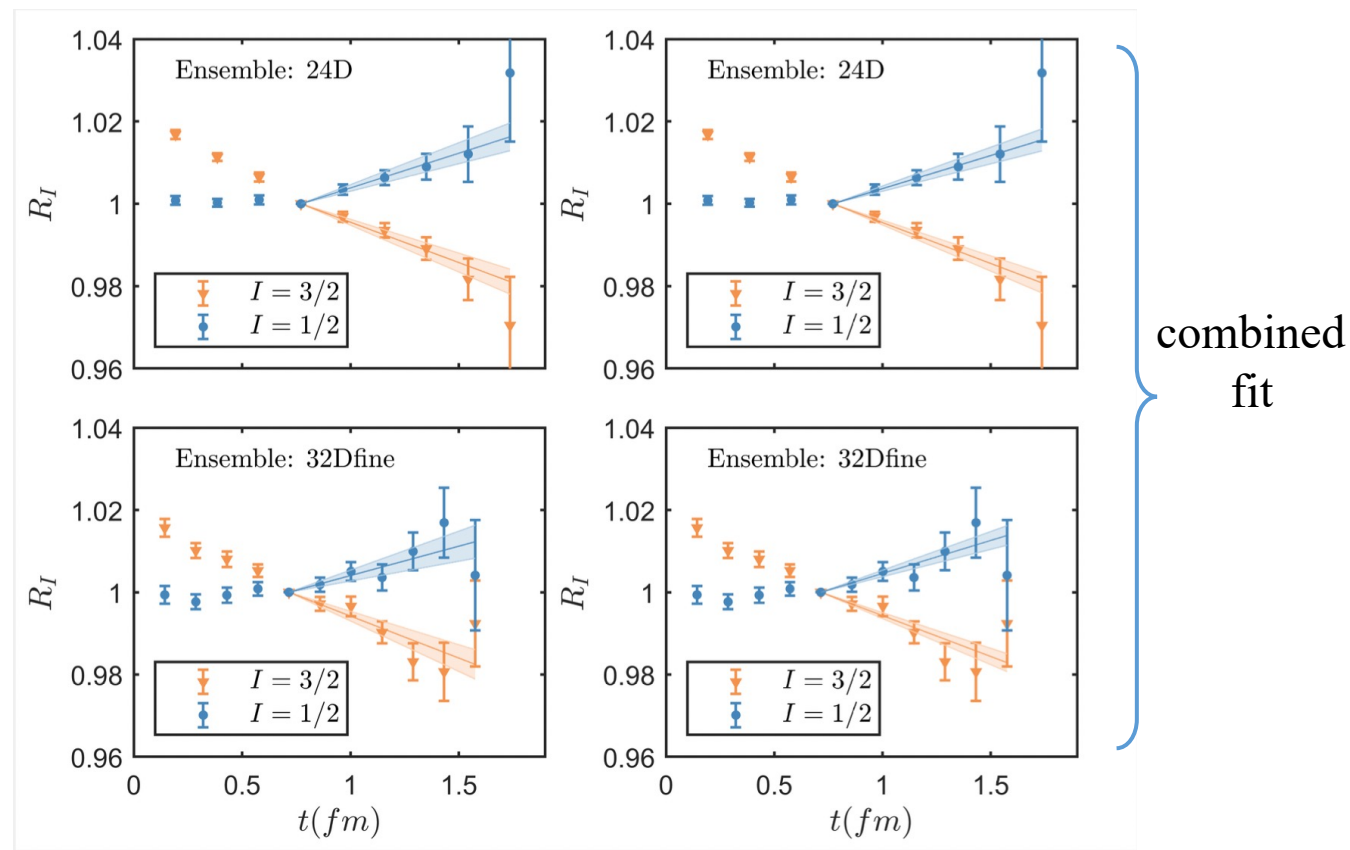
$$= \frac{A_{N\pi}}{A_N A_\pi} \frac{e^{-E_{N\pi}t}}{e^{-(M_N+M_\pi)t}}$$

$$\approx R_0(1 - \Delta E t)$$

with $\Delta E = E_{N\pi} - M_N - M_\pi$

➤ Scattering for different isospin channel

- $I = 1/2$, $\Delta E < 0$, attractive interaction
- $I = 3/2$, $\Delta E > 0$, repulsive interaction



Results using data at threshold

$$a_0^{1/2} m_\pi = 0.157(31), a_0^{3/2} m_\pi = -0.104(18)$$

$$\text{ETMC [arXiv: 2307.12846]} a_0^{3/2} m_\pi = -0.13(4)$$

Analysis based on cross section and πH , πD spectrum

$$a_0^{1/2} m_\pi = 0.170(2), a_0^{3/2} m_\pi = -0.087(2)$$

M. Hoferichter et al, PLB 843 (2023) 138001

$\sim 1\sigma$

Matrix elements of $N\gamma \rightarrow N\pi$

- Normalization for ${}_I\langle N\pi | J_i^{I'} | N \rangle$

$$R = \frac{C_{NJN\pi}(t_1, t_2)}{C_{N\pi}(t_1 + t_2)} \times \sqrt{\frac{C_N(t_1)C_{N\pi}(t_2)C_{N\pi}(t_1 + t_2)}{C_{N\pi}(t_1)C_N(t_2)C_N(t_1 + t_2)}}$$

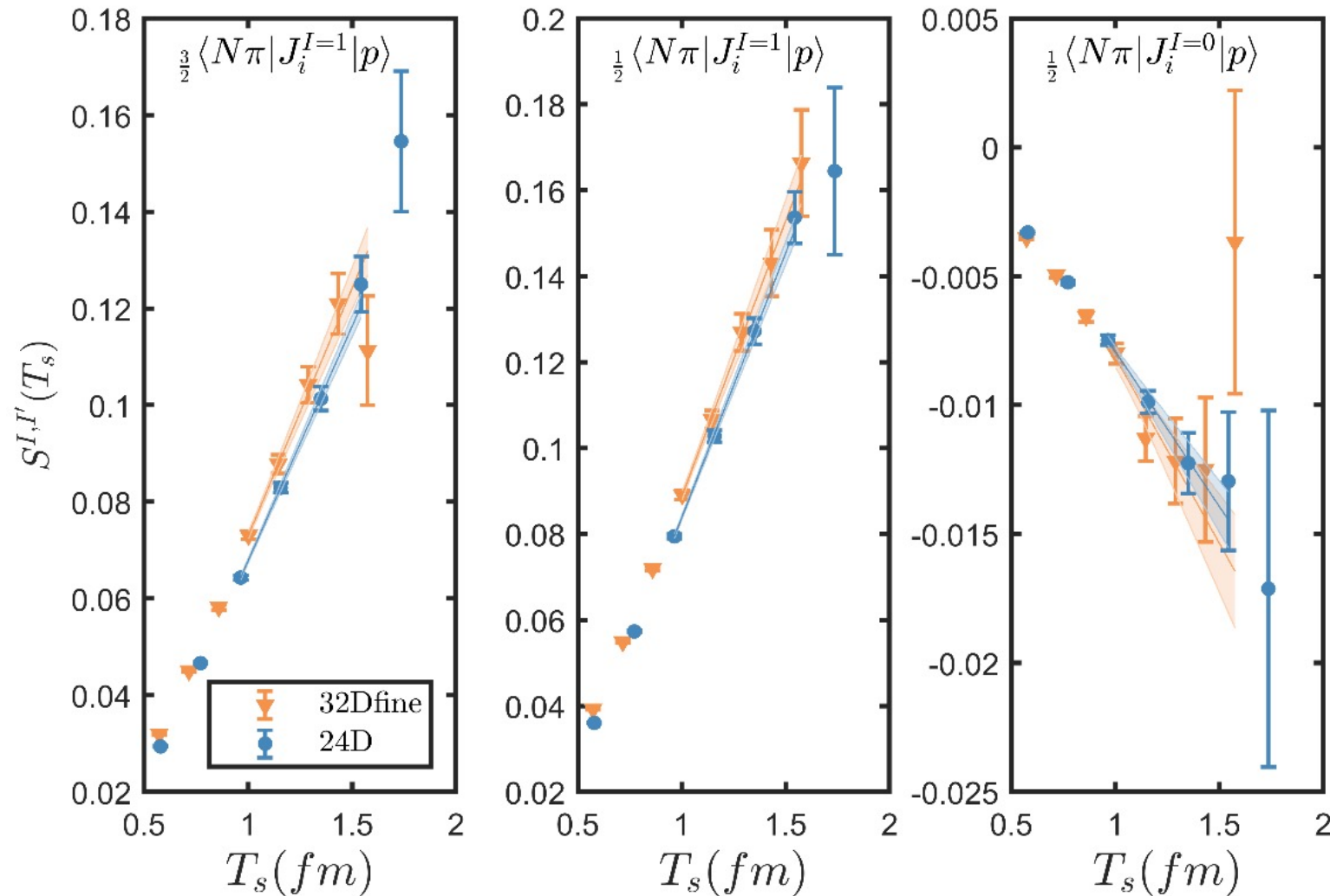
- Summed insertion

Maiani L. NPB, 293, 420(1987)

$$S(T_s) = \sum_{t_1+t_2=T_s} R(t_1, t_2) \xrightarrow{T_s \rightarrow \infty} c_0 + \frac{1}{\sqrt{2M}} {}_I\langle N\pi | J_i^{I'} | N \rangle \cdot T_s$$

- Linear fit $S(T_s)$ with T_s to extract

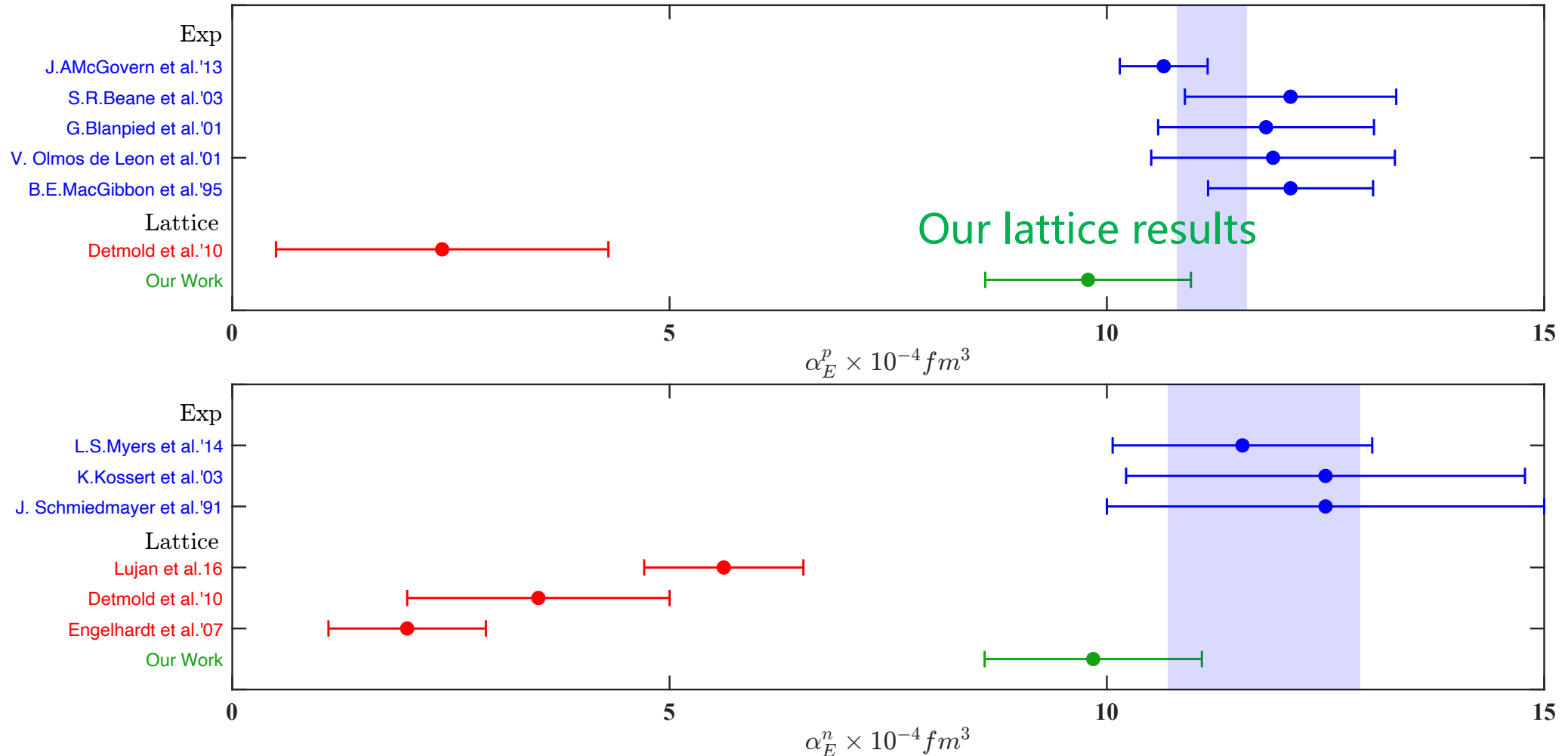
$N\pi$ at the threshold



Numerical results

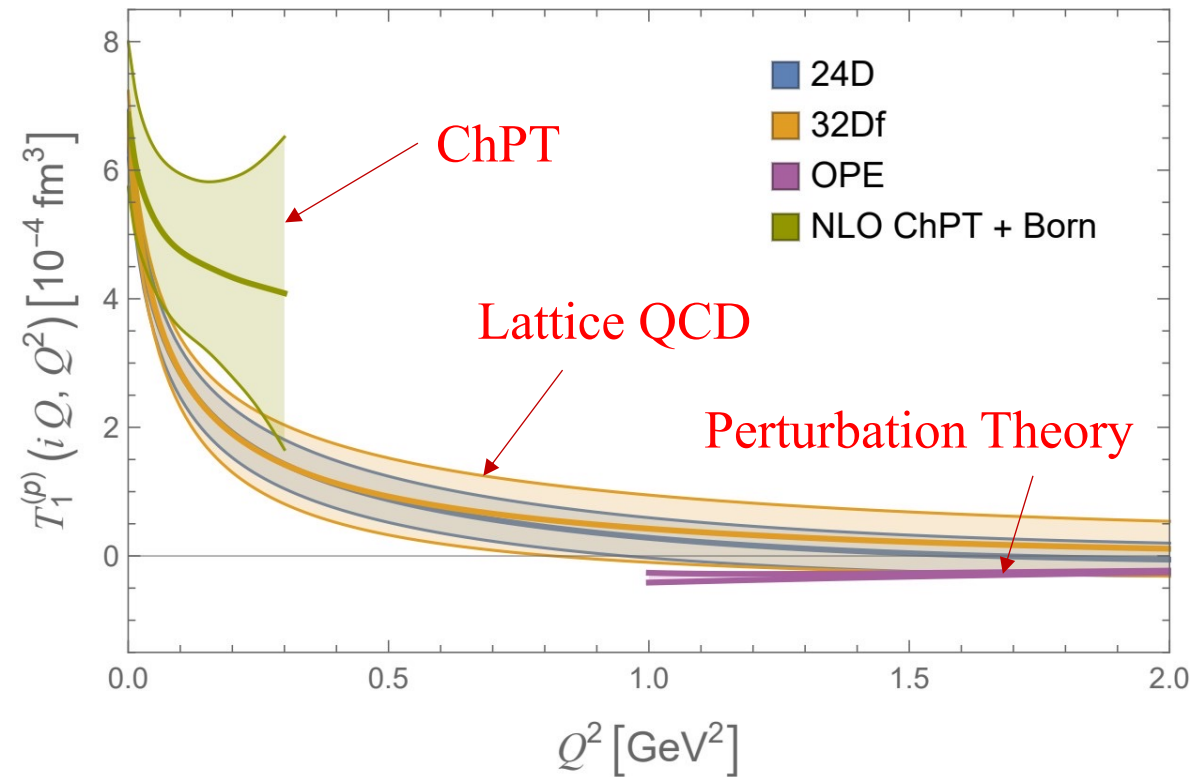
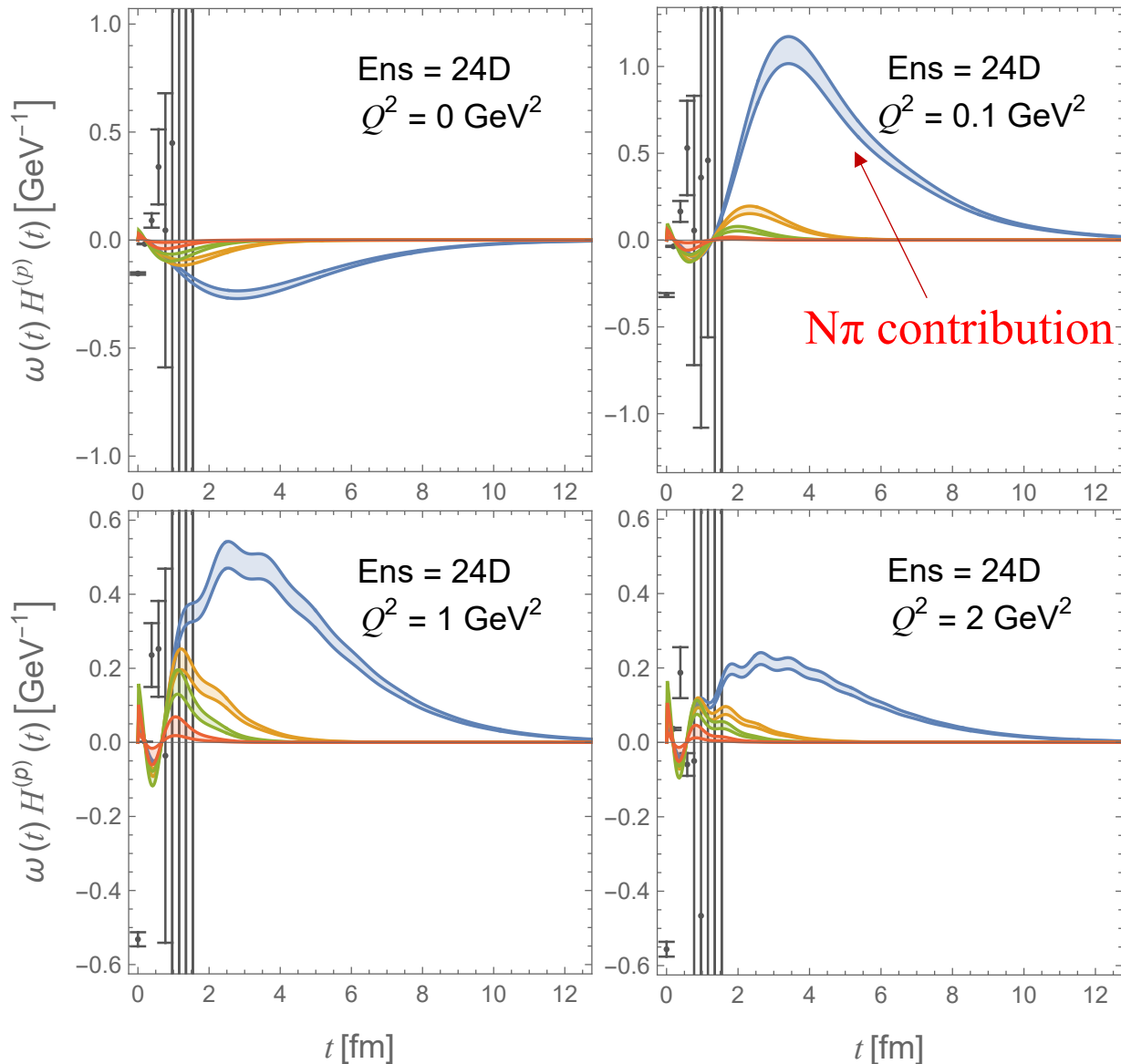
- Need to calculate $N\pi$ scattering and π -production, in total **3** times of workload
- Reconstruction of contributions from $N\pi$ states – **60%** for proton & **90%** for neutron

X. Wang, Z. Zhang, X. Cao, XF, et. al. PRL 133 (2024) 141901



Lattice QCD computation of subtraction function

— 4pt $N\pi, n=0$ $N\pi, n=1$ $N\pi, n=2$ $N\pi, n=3$

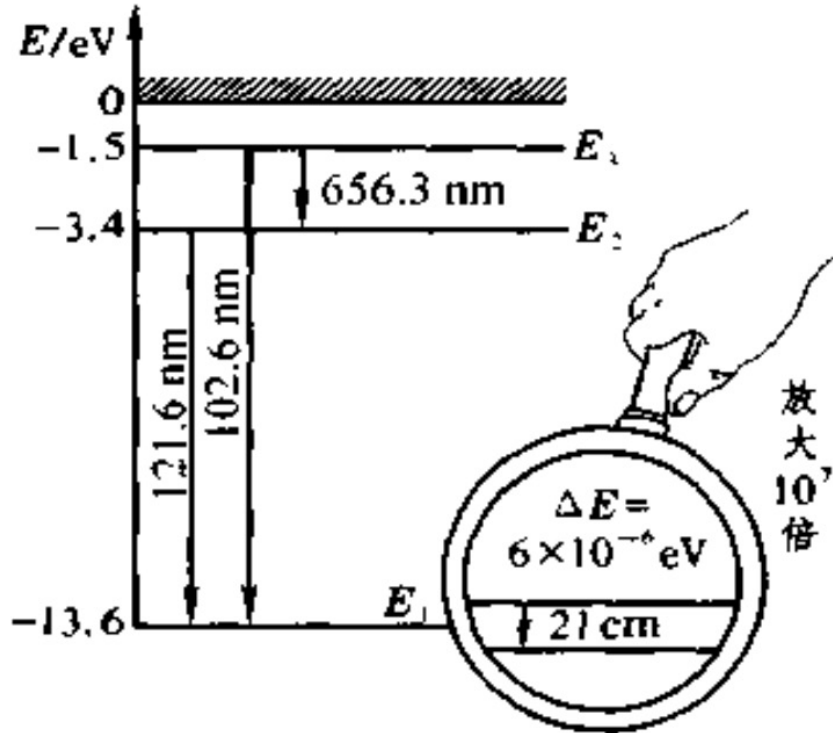


Y. Fu, XF, L. Jin, et.al PRL 134 (2025) 071903

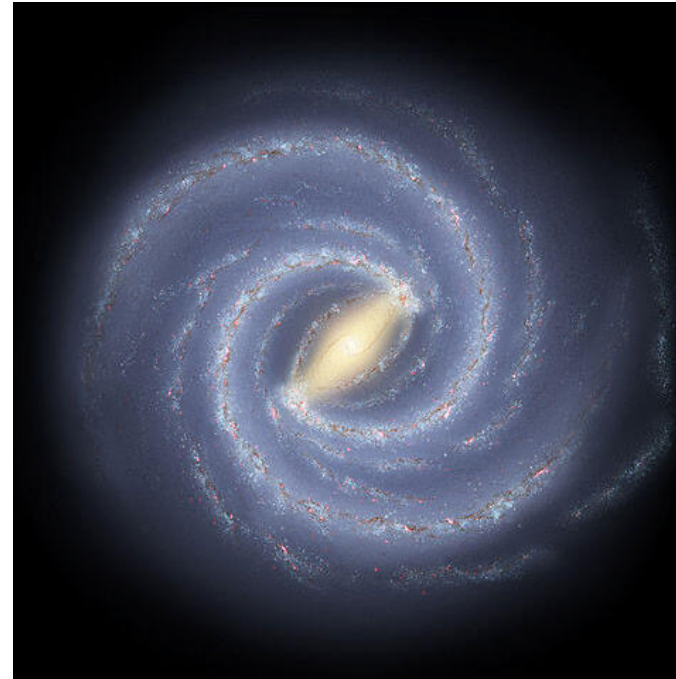
- Reconstruction $N\pi$ contribution is essential
- LQCD provide accurate input for subtraction function
- Joint approach: uncertainty reduced by ~ 4 times compared to full lattice results

Outlook: from Lamb shift to hyperfine splitting

- Hyperfine splitting arises from proton magnetic moment interacting with the magnetic field generated by the lepton



- Hydrogen 21cm line comes from hyperfine splitting



- It marked the birth of spectral-line radio astronomy
- In 1952 the first maps of hydrogen in the Galaxy were made and the spiral structure of the Milky Way was revealed

- Largest theoretical uncertainty to determine hyperfine splitting also originates from TPE
- Lamb shift is related to charge radius, while hyperfine splitting is related to proton magnetic moment. Thus in many aspects e.g. computational method and IR structure, they're quite different.



Another interesting theoretical research work!